

# White-light emission from organic aggregates: a review

Jianyu Zhang,<sup>a,†</sup> Xueqian Zhao,<sup>a,†</sup> Hanchen Shen,<sup>a</sup> Jacky W. Y. Lam,<sup>a</sup> Haoke Zhang,<sup>b,c,d,\*</sup> and Ben Zhong Tang<sup>a,d,e,f,\*</sup>

<sup>a</sup>The Hong Kong University of Science and Technology, Department of Chemistry, Hong Kong Branch of Chinese National Engineering Research Center for Tissue Restoration and Reconstruction, and Guangdong-Hong Kong-Macau Joint Laboratory of Optoelectronic and Magnetic Functional Materials, Clear Water Bay, Kowloon, Hong Kong, China

<sup>b</sup>Zhejiang University, MOE Key Laboratory of Macromolecular Synthesis and Functionalization, Department of Polymer Science and Engineering, Hangzhou, China

<sup>c</sup>ZJU-Hangzhou Global Scientific and Technological Innovation Center, Hangzhou, China

<sup>d</sup>South China University of Technology, Guangdong Provincial Key Laboratory of Luminescence from Molecular Aggregates, Guangzhou, China

<sup>e</sup>The Chinese University of Hong Kong, Shenzhen Institute of Aggregate Science and Technology, School of Science and Engineering, Shenzhen, China

<sup>f</sup>AIE Institute, Guangzhou Development District, Guangzhou, China

**Abstract.** White light, which contains polychromic visible components, affects the rhythm of organisms and has the potential for advanced applications of lighting, display, and communication. Compared with traditional incandescent bulbs and inorganic diodes, pure organic materials are superior in terms of better compatibility, flexibility, structural diversity, and environmental friendliness. In the past few years, polychromic emission has been obtained based on organic aggregates, which provides a platform to achieve white-light emission. Several white-light emitters are sporadically reported, but the underlying mechanistic picture is still not fully established. Based on these considerations, we will focus on the single-component and multicomponent strategies to achieve efficient white-light emission from pure organic aggregates. Thereinto, single-component strategy is introduced from four parts: dual fluorescence, fluorescence and phosphorescence, dual phosphorescence with anti-Kasha's behavior, and clusteroluminescence. Meanwhile, doping, supramolecular assembly, and cocrystallization are summarized as strategies for multicomponent systems. Beyond the construction strategies of white-light emitters, their advanced representative applications, such as organic light-emitting diodes, white luminescent dyes, circularly polarized luminescence, and encryption, are also prospected. It is expected that this review will draw a comprehensive picture of white-light emission from organic aggregates as well as their emerging applications.

Keywords: aggregate; white-light emission; aggregation-induced emission; organic; mechanism.

Received Sep. 29, 2021; revised manuscript received Nov. 7, 2021; accepted for publication Dec. 2, 2021; published online Dec. 30, 2021.

© The Authors. Published by SPIE and CLP under a Creative Commons Attribution 4.0 International License. Distribution or reproduction of this work in whole or in part requires full attribution of the original publication, including its DOI.

[DOI: [10.1117/1.AP.4.1.014001](https://doi.org/10.1117/1.AP.4.1.014001)]

## 1 Introduction

Light has illuminated the world and promoted the development of society, especially since Thomas Edison invented incandescent lightbulbs in 1879. Natural sunlight contains different wavelengths of light within the visible spectrum and finally

shows white color. It affects the metabolism of humans and controls the circadian rhythm of organisms.<sup>1</sup> To mimic natural sunlight, steps on the exploration of white-light luminescent materials have never stopped. They have exhibited a wide range of lighting applications in illumination, industry automotive, information communication, and luminescent dyes. Compared with traditional incandescent lightbulbs and inefficient mercury-discharge-based fluorescent lamps, solid-state sources such as LEDs exhibit advantages such as high efficacy, small size, color stability, controllability, and variability, thus attracting increasing

\*Address all correspondence to Haoke Zhang, [zhanghaoke@zju.edu.cn](mailto:zhanghaoke@zju.edu.cn); Ben Zhong Tang, [tangbenz@cuhk.edu.cn](mailto:tangbenz@cuhk.edu.cn)

<sup>†</sup>These authors contributed equally to this work.

attention from scientists and industries.<sup>2-4</sup> Being different from traditional light sources with monochromatic light, white-light emitters should produce polychromatic lights simultaneously, which usually requires them to have di-, tri-, or tetrachromatic sources.<sup>2,3,5</sup> For example, white-light LEDs with high brightness and durability could be realized by synergistically combining traditional LED with three primary colors (e.g., blue InGaN LED, green InGaN LED, and red GaAlAs LED).<sup>6</sup> Other strategies based on ultraviolet/blue LED plus phosphors have been successfully utilized.<sup>7-9</sup> The past several decades have witnessed a prosperous era in the generation and commercialization of white-light emitters based on inorganic semiconductor p-n junction diodes and phosphors.

It is acknowledged that some organometallic aggregates are also good candidates for luminescence and realizing white-light emission with high efficiency.<sup>10,11</sup> However, compared with inorganic and organometallic materials with rare-earth elements, pure organic compounds show better processability, flexibility, structural diversity, environmental friendliness, etc., which endows them with promising applications in advanced smart devices.<sup>12</sup> However, many organic luminophores suffer the severe aggregation-caused quenching (ACQ) effect, which strongly impedes their practical applications in the aggregate and solid states.<sup>13,14</sup> Meanwhile, most of them are monochromatic, so it is difficult to realize white-light emission from single-component organic emitters, which require intricate multilayered device fabrications. The above hindrances block the generation and utilization of white light from organic luminescent materials for decades. In 2001, Tang et al. coined the photophysical concept of aggregation-induced emission (AIE) which brought a new perspective for molecular behavior in the aggregate state.<sup>15</sup> AIE refers to the photophysical phenomenon that some certain molecules are nonemissive in the isolated solution state but would show strong photoluminescence (PL) in the aggregate or solid state.<sup>16-18</sup> In the past two decades, AIE has

motivated much research on aggregate science from fundamental mechanisms to advanced applications and promoted the diagram shift from molecular science to aggregate science.<sup>19-25</sup> The emergences and changes originating from aggregation are beyond enhanced PL intensity. Some new phenomena that do not exist in the single molecule emerge in the aggregate state, such as room-temperature phosphorescence (RTP), clusteroluminescence, and mechanoluminescence.<sup>16,26</sup> From this consideration, organic aggregates showing the AIE effect are also promising to provide a new insight on pursuing white-light emission in terms of strategies and applications.<sup>27-29</sup> Some luminogens with the AIE effect (AIEgens) with flexible structures can emit polychromatic colors simultaneously in the aggregate state, achieving the requirements for white light. In addition, the solid-state form and high efficiency of AIEgens are beneficial to practical applications.<sup>30-33</sup> However, only a few compounds were reported as organic white-light emitters, and few general methods or strategies are constructed as the guidance for achieving solid-state white light.<sup>34</sup> Hence, it requires in-depth understanding of the principles and mechanisms behind photophysical behaviors of organic aggregates to generate white-light emission.

In this review, from the mechanistic perspective, we focus on the fundamental strategies to achieve efficient white-light emission from pure organic aggregates, which are summarized from single-component and multicomponent systems, respectively (Fig. 1). Single-component strategies include dual fluorescence from two singlet states, fluorescence and phosphorescence, dual phosphorescence with anti-Kasha's behavior, and clusteroluminescence. Subsequently, doping, supramolecular assembly, and cocrystallization are introduced as strategies for multicomponent systems. Finally, some emerging applications of organic emitters with white-light emission are highlighted. It is expected that this review will draw a comprehensive picture for white-light emitters of organic aggregates.

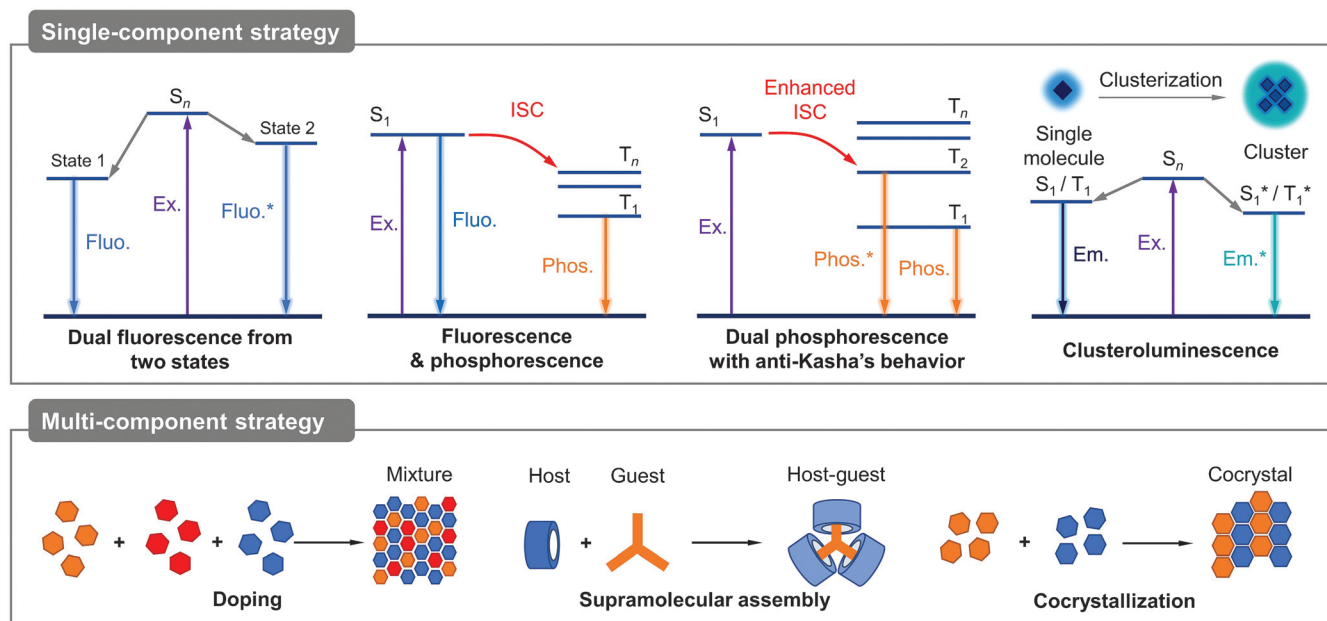


**Fig. 1** General scheme of single-component and multicomponent strategies to achieve white-light emission from organic aggregates. Ex., excitation; Fluo., fluorescence; Phos., phosphorescence; Em., emission; ISC, intersystem crossing.

## 2 Single-Component Strategy

Mixing two or three compounds with primary colors together is a simple method to construct multicolor emission with the merits of high-quality white light, high efficiency, and mature fabrication techniques. However, its performance is like a double-edged sword that brings the problems of phase separation, high casting cost, and unstable emission color. In contrast, single-molecule systems with polychromic emission are ideal candidates to achieve white-light emission. Several single-molecule white-light emitters have been reported in solution conditions.<sup>35–37</sup> With the help of the AIE effect, it is possible for organic luminogens to exhibit efficient white-light emission in the aggregate or solid state with high color quality, stability, and controllability. In this section, various reported design principles and mechanisms to achieve white-light emission from single-component organic aggregates will be discussed.

### 2.1 Dual Fluorescence from Two States

When one molecule is excited to the higher excited state, it will quickly relax to the lowest excited state through internal

conversion (IC) and then return to the ground state through competitively radiative and nonradiative decay channels, which is illustrated by Kasha's rule.<sup>38</sup> For this reason, most molecules only have one fluorescent emissive state and show monochromic emission. However, the structural features of some molecules enable two or more emissive states to be presented and balanced at the same time, which realize polychromic emission from two or more fluorescent states following Kasha's rule. According to the region of electron distribution before and after excitation, the common origins of fluorescence are usually divided into locally excited (LE) and charge transfer (CT) states. The former refers to the same electron distribution after excitation, while the latter indicates an obvious region change of electron distribution. Here, three common cases, namely, LE and CT, dual LE, and dual CT fluorescence for white-light emission are introduced (Fig. 2). It should be noticed that dual fluorescence can also be generated from some special molecules with excited-state intramolecular proton transfer,<sup>42–44</sup> structural isomerization,<sup>45</sup> and excimers,<sup>46</sup> which have been summarized by some reviews.<sup>34,47</sup>

When two chromophores that do not show obvious electron-donating or electron-withdrawing features are connected, they

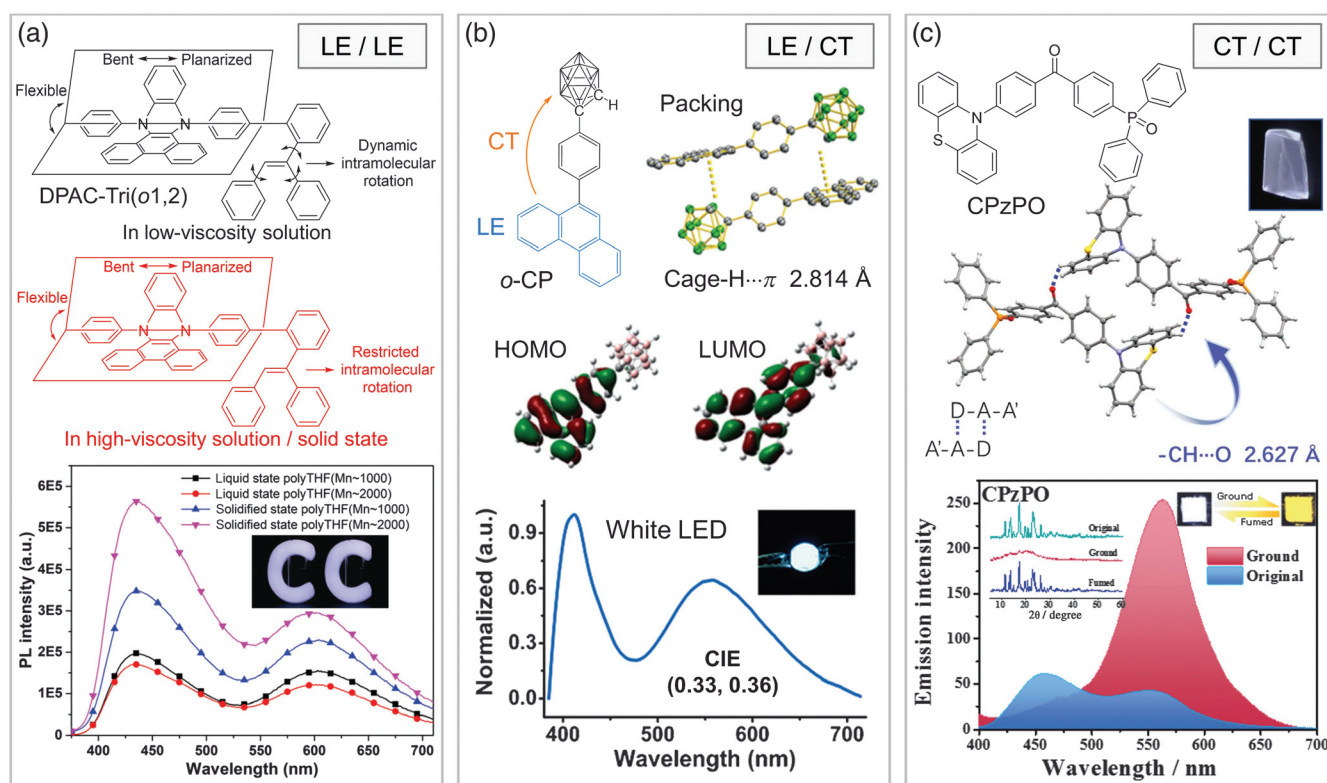


**Fig. 2** Schematic illustration of three types of dual emissions from two fluorescent states. LE, locally excited; CT, charge transfer. (a) (Upper panel) The molecular conformations and photo-physical behaviors of DPAC-Tri(o1,2) in a low-viscosity and high-viscosity solution/solid state; (lower panel) PL spectra of DPAC-Tri(o1,2) in different states of polytetrahydrofuran (polyTHF); (inset) fluorescent photo of DPAC-Tri(o1,2) (concentration: 10<sup>-5</sup> mol/L) in solidified polyTHF with an Mn of 2000 Da. The excitation wavelength is 365 nm. Figures are reproduced with permission from Ref. 39. (b) (Upper panel) Chemical structure, crystal packing, and calculated HOMO-LUMO distribution of o-CP; (lower panel) PL spectra and photo of a white LED based on o-CP. Figures are reproduced with permission from Ref. 40. (c) (Upper panel) Chemical structure, crystal packing of CPzPO; PL spectra and photo of CPzPO before and after grinding. Figures are reproduced with permission from Ref. 41.

may emit two independent lights from their corresponding LE states after photoexcitation. For example, a typical saddle-shaped compound, *N,N*-disubstituted-dihydrodibenzo[*a,c*]phenazines (DPAC), and a typical AIEgen triphenylethylene (TPE) were utilized to construct the compound DPAC-Tri(*o*1,2) [Fig. 2(a)].<sup>39</sup> The moiety of DPAC was flexible so that it displayed planarized conformation in the ground state and became bent in the excited state, which was unsusceptible to the surrounding environment. However, the other part of the TPE exhibited dynamic intramolecular rotation in the isolated state and restricted intramolecular rotation in the aggregate state. Therefore, in a low-viscosity solution, organ-red emission from the DPAC part was observed while another blue light from the TPE was quenched. In contrast, bright white light was achieved from dual LE emission in the high-viscosity solution or solid state, which contained both orange-red and blue colors from two separated fluorogens, respectively. Furthermore, polytetrahydrofuran (polyTHF) was utilized as a “solvent” to powerfully restrict intramolecular motion. Hence, the blue emission with a wavelength of 435 nm was strongly enhanced when the state of the polyTHF changed from liquid to solid. A solid model with two letters of “CC” was made accordingly with a cold-white color and an International Commission on Illumination (CIE) coordinate of (0.28, 0.25) [Fig. 2(a)].

If there is an equilibrium between parent LE and CT states, dual fluorescence can also be achieved. Hence, it requires a moderate strength between a donor–acceptor (D-A) pair to balance the strength of LE and CT and further realize white light.<sup>48–50</sup> The first example of such a dual-emission emitter was originally reported in a donor–acceptor compound named 4-*N,N*-dimethylaminobenzonitrile in 1959.<sup>51</sup> Tu et al. reported a single-component white-light emitter *o*-CP where the phenanthrene acted as the donor and the carborane group played as the acceptor [Fig. 2(b)].<sup>40</sup> Due to the weak electron-withdrawing ability of the carborane unit, one blue emission from the LE state located at phenanthrene and the other yellow emission with the CT feature were achieved simultaneously in the crystalline phase. In addition, with the help of multiple intermolecular hydrogen bonds (Cage-H $\cdots\pi$ ), intramolecular motions and non-radiative decay of *o*-CP were suppressed in the solid state, resulting in high-purity white light with an absolute quantum yield of 46% and a CIE coordinate of (0.33, 0.36). A white-light emitting device was also fabricated with a brightness as high as  $1.4 \times 10^4$  cd m<sup>-2</sup> under a low operating voltage of 4.0 V.

Further increasing the strength of the electron-donating and electron-withdrawing abilities between a D-A pair, the emission from the CT state becomes dominant without any LE feature.<sup>52,53</sup> Specifically, polychromic emission from CT states may be observed if two or more different D-A pairs are presented. Chi et al. reported an asymmetrical compound CPzPO based on diphenylsulfone, diphenylketone, and diphenylphosphine oxide, which showed a donor–acceptor–acceptor conformation [Fig. 2(c)].<sup>41</sup> It showed only one blue emission (~460 nm) in a dilute solution, which was generated from the intramolecular CT between phenothiazine and ketone moieties. However, apart from the blue emission, its crystal displayed another low-energy emission band at 568 nm. Through single-crystal analysis, excitation spectrum measurement, and blending and grinding experiments, the long-wavelength band was assigned to the intermolecular CT from phenothiazine moiety to ketone moiety with the assistance of intermolecular hydrogen bonds (-CH $\cdots$ O = 2.627 Å). As a result, CPzPO emitted pure white color with a CIE

coordinate of (0.31, 0.32) assisted by synergistic intramolecular and intermolecular CT states.

## 2.2 Fluorescence and Phosphorescence

Traditionally, phosphorescence of pure organic molecules has been disregarded since it is too weak to be observed at room temperature and triplet excitons are easily quenched. According to the Jablonski diagram, to achieve RTP with high efficiency, efficient intersystem crossing (ISC) from singlet to triplet states, suppressed nonradiative decay or quenching processes of the triplet states, and fast phosphorescent decay from triplet to ground states are prerequisites.<sup>54</sup> With the development of aggregate science, research on RTP from organic aggregates rapidly developed with various systems, strategies, and multiple functionalities.<sup>55–58</sup>

Accompanying fluorescence from the singlet state, the emission from the triplet state as phosphorescence provides another focus on white light from single-component organic aggregates. The key to this strategy is to directly manipulate the strength of ISC and further adjust the equilibrium between singlet and triplet excitons after photoexcitation.<sup>59,60</sup> Heavy atoms are usually used to enhance the weak ISC ability of organic molecules to promote triplet excitons.<sup>61,62</sup> For instance, TPO-Br was successfully synthesized that showed blue fluorescence and strong yellow RTP in the solid state (Fig. 3).<sup>63</sup> The pure TPO-Br film prepared by spin-coating exhibited high-quality white light with a CIE coordinate of (0.32, 0.33) [Fig. 3(b)], which was very close to the pure white color of (0.33, 0.33) defined by CIE in 1931.<sup>64</sup> Single-crystal structure analysis suggests that, apart from twisted phenyl rings around the oxazole core, two Br anions closely located on both sides of the positively charged oxazoliums with distances of 3.494 and 3.601 Å, respectively [Fig. 3(c)]. This conformation and anion– $\pi^+$  interactions blocked the strong intermolecular interactions and promoted efficient emission in the aggregate state. The small energy difference between S<sub>1</sub> and T<sub>3</sub>/T<sub>4</sub> states (0.18 eV) and large spin-orbit coupling assisted by the external heavy-atom effect of Br anions ensured the strong ISC for RTP [Fig. 3(d)]. As a result, the balance between fluorescence and phosphorescence produced the dual emission and final white-light emission.

The strength of ISC and equilibrium between the singlet and triplet states are also indirectly controlled by other methods, such as oxidation degree of thianthrene,<sup>65</sup> intermolecular hydrogen bonding,<sup>66</sup> halogen bonding,<sup>67,68</sup> one-dimensional  $\pi - \pi$  stacking,<sup>69,70</sup> and oxygen/nitrogen heteroatom with ( $n, \pi^*$ ) transition.<sup>71,72</sup> These examples provide prosperous methods to modulate excited-state features and harvest efficient white-light emission from pure organic aggregates.

## 2.3 Dual Phosphorescence with Anti-Kasha's Behavior

A rare but interesting phenomenon is that molecules can emit light from a higher excited state (e.g., S<sub>*n*</sub> and T<sub>*n*</sub>, *n* ≥ 2), which violates Kasha's rule, and was originally discovered in azulene in 1955.<sup>73</sup> In general, after being excited to the higher excited state, excitons quickly relax to the lowest excited state (S<sub>1</sub> or T<sub>1</sub>) through IC.<sup>74,75</sup> Hence, it is scarce to obtain emissions from higher excited states. There are a few studies that reported and strictly verified this unusual anti-Kasha's emission from multiple excited singlet states.<sup>76,77</sup>

As a special case to traditional molecules with one emission peak of RTP, pure phosphorescence with anti-Kasha's behavior

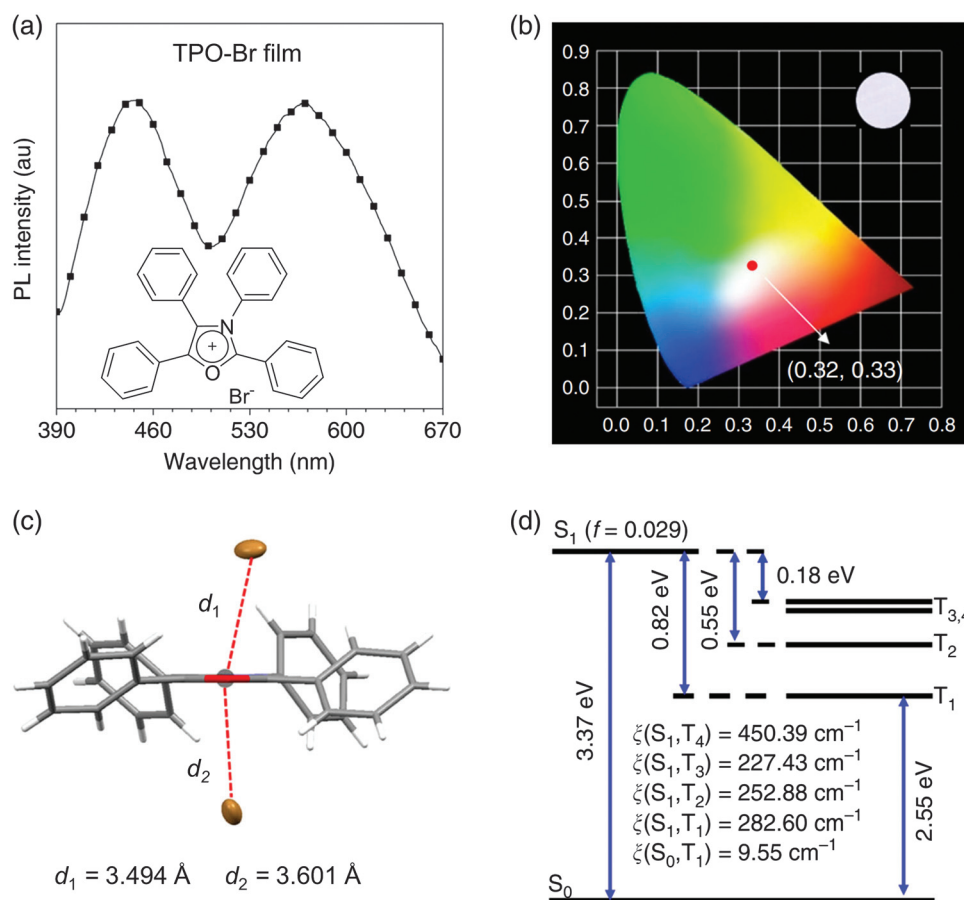


**Fig. 3** (a) PL spectrum of organic salt, TPO-Br, under room temperature; (inset) chemical structure of TPO-Br. (b) The CIE chromaticity coordinate of emission from TPO-Br film. (c) Single-crystal structure of TPO-Br and its anion- $\pi^+$  interactions. (d) The theoretically calculated energy diagram and spin-orbit couplings ( $\xi$ ) between singlet and triplet states of TPO-Br based on the optimized ground-state geometry using the ONIOM method. Figures are reproduced with permission from Ref. 63.

provides more complicated photophysical processes and mechanistic value.<sup>78</sup> Dual emission of phosphorescence also indicates the possibility to obtain white-light emission from single-component systems. In principle, there are two ways to achieve such anti-Kasha's phosphorescence. (1) Large energy difference between the higher excited state and  $T_1$  so the higher triplet state does not involve the  $T_1$ , which suppresses the rate of IC. (2) The higher triplet state and  $T_1$  are vibronically mixed or thermally equilibrated with energy proximity or small energy difference, and the radiative rate from the higher triplet state is much faster than that from  $T_1$ .<sup>79,80</sup> As a result, dual phosphorescence can be achieved from two triplet states. With the help of the carbonyl group and heavy halogen atom to greatly strengthen ISC, Tang et al. studied a pure organic compound, CIBDBT, as the first example of white-light emitter showing pure phosphorescence with anti-Kasha's behavior.<sup>81</sup> As shown in Fig. 4(a), the powder of CIBDBT showed white and yellow colors with and without UV illumination, respectively. The PL spectra indicated two emission peaks located at 467 and 551 nm with a white-light CIE coordinate of (0.33, 0.35) [Figs. 4(b) and 4(c)]. To verify the origin of the dual emission, variable-temperature lifetime was investigated. The blue and yellow emission showed

lifetimes of 0.41 and 123.4 ms at room temperature (300 K), respectively, and their lifetime increased with the decreased temperature from 300 to 50 K [Figs. 4(d) and 4(e)]. These results support their nature of phosphorescence. The calculated energy gap between  $T_2$  and  $T_1$  was 0.27 eV, indicating the nature of thermally mixed two states. The higher-energy  $T_2$  showed an ( $n, \pi^*$ ) transition character, while the lower-energy  $T_1$  was dominant with a ( $\pi, \pi^*$ ) transition character. The transition oscillator strength ( $f$ ) of  $T_2$  ( $1.08 \times 10^{-6}$ ) is much larger than that of  $T_1$  ( $0.37 \times 10^{-6}$ ), leading to an experimental short lifetime of  $T_2$  and long lifetime of  $T_1$  [Fig. 4(f)]. As a result, two radiative decay channels generated the white-color emission through balancing two emissions of phosphorescence with anti-Kasha's behavior.

#### 2.4 Clusteroluminescence

Being different from traditional emissive compounds based on through-bond conjugation (e.g., double bonds, triple bonds, and aromatic rings), many nonconjugated or poorly conjugated molecules, such as polystyrene and maleimide, also emit visible light in the aggregate state although they are nonemissive in

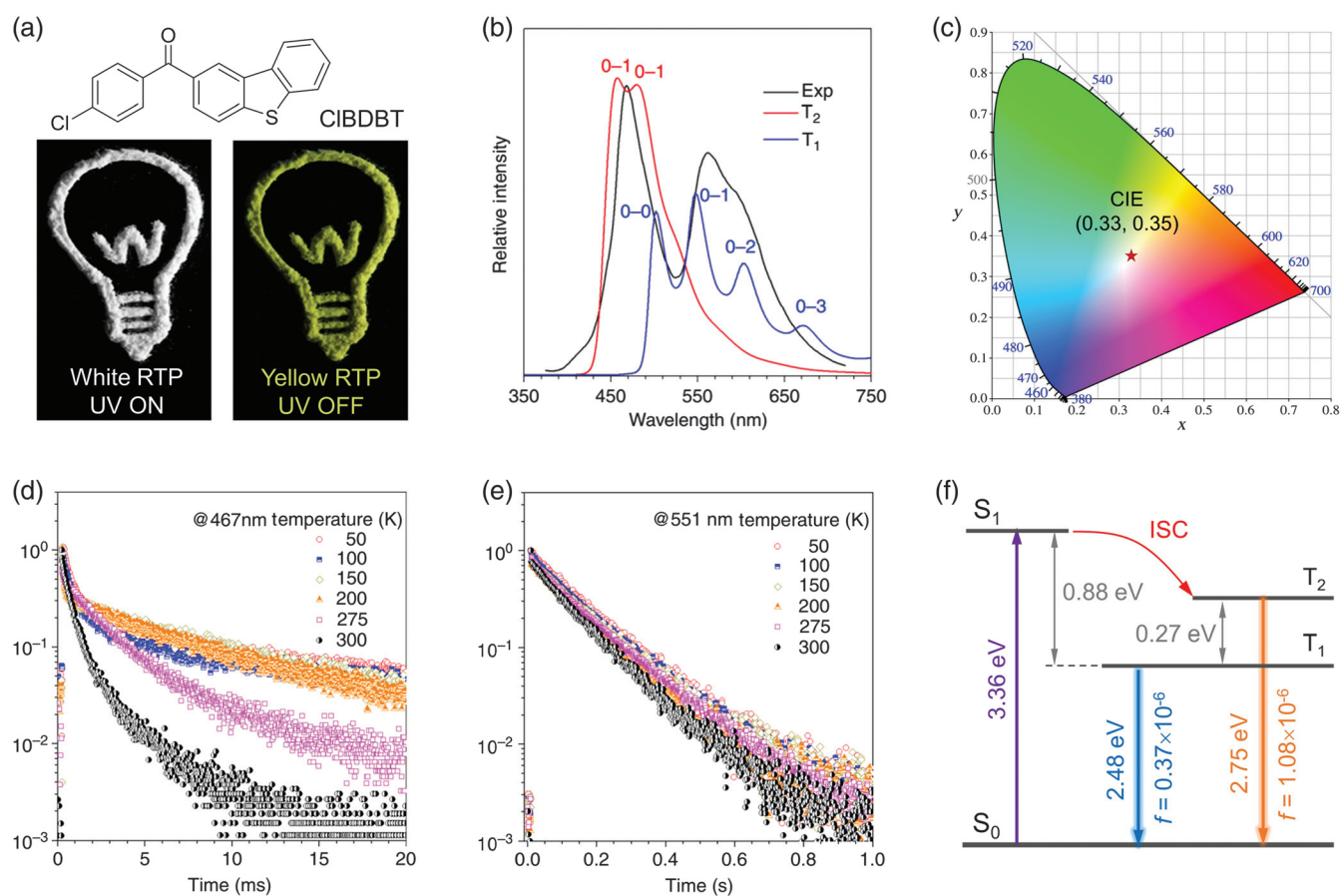


**Fig. 4** (a) Chemical structure of CIBDBT and luminescent photos of its powder with or without irradiation of 365 nm UV lamp. (b) Experimental and calculated PL spectra of CIBDBT powder. (c) The CIE chromaticity coordinate of emission from solid CIBDBT. (d) PL decay curve of the short-wavelength emission ( $\lambda_{em} = 467$  nm) under different temperatures. (e) PL decay curve of the long-wavelength emission ( $\lambda_{em} = 551$  nm) under different temperatures. The excitation wavelength is 365 nm. (f) Adiabatic energy diagram and oscillator strength between two triplet states and ground state calculated at (TD) B3LYP/6-31(d)/GAFF level. Figures are reproduced with permission from Ref. 81.

the solution.<sup>82–84</sup> This unconventional photophysical process is termed as clusterization-triggered emission (CTE) and the corresponding emission is known as clusteroluminescence.<sup>85,86</sup> Previous studies suggested that strong intermolecular and intramolecular interactions play vital roles in clusteroluminescence. Electronic delocalization and coupling between electron-rich groups (e.g., carbonyl, hydroxyl, and sulfhydryl groups) can generate new emissive species and stabilize excitons to produce such clusteroluminescence.<sup>58,87</sup> These new species usually produce emission with a longer wavelength than the intrinsic short-wavelength emission of the electron-rich groups from through-bond conjugation.

With the idea of clusteroluminescence, it is possible to produce multicolor emission from such nonconjugated compounds based on their different through-space interaction (TSI) properties in the clustered state, which could eventually achieve white-light emission.<sup>88–91</sup> Zhang et al. synthesized a linear siloxane-based poly(hydroxyurethane) (PHU) that contained carbonyl, hydroxyl groups, and ether bonds [Fig. 5(a)].<sup>92</sup> The twisted and entangled chains in the aggregate state allowed these electron-rich groups to approach each other and formed electronic

delocalization through multiple hydrogen bonds and ( $n, \pi^*$ ) transition. Therefore, PHU film fabricated by rotary coating showed excitation-dependent and strong visible-range emission with 52% of blue-to-red color within the whole spectra, suggesting the high conversion efficiency from UV light to white-light emission [Fig. 5(b)]. As discussed above, this visible-range emission originated from TSI of delocalized electrons, which was assisted by multiple intermolecular and intramolecular interactions. As expected, the counterpart of PHU without side hydroxyl groups was nonemissive, suggesting the importance of such electron-rich groups to clusteroluminescence. Fortunately, a white-light emitter with a CIE coordinate of (0.33, 0.38) was achieved when the PHU was coated on a 365-nm UV lamp. Its emission spectrum covered the whole visible range with two peaks at 476 and 550 nm, which was attributed to the CTE from PHU clusters with different TSI [Figs. 5(c) and 5(d)]. It is noteworthy that this white-light emitter was comparable with a commercial white LED in terms of its correlated color temperature of 5681 K, high luminance of 8222  $\text{cd m}^{-2}$ , and color rendering index of 83.

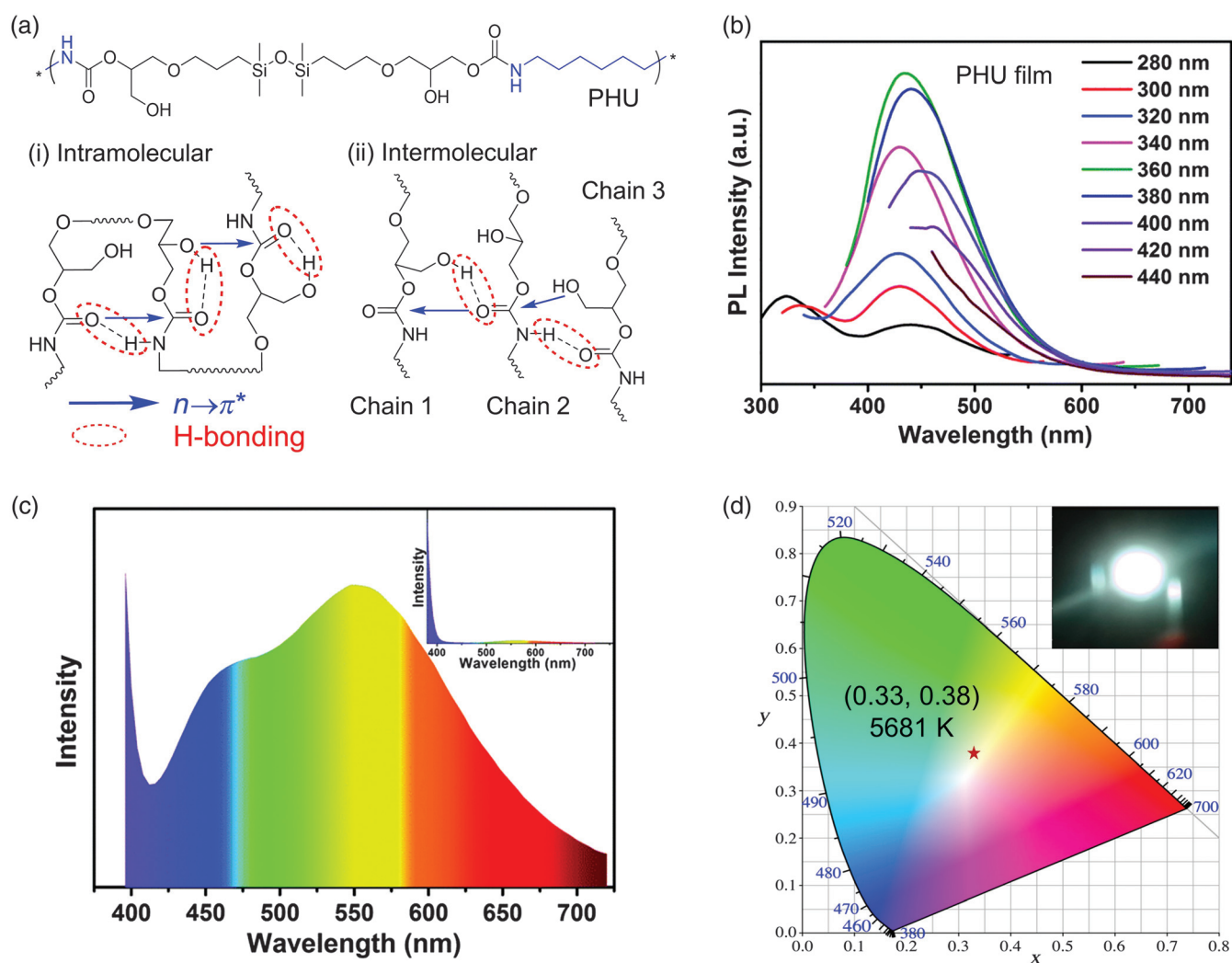


**Fig. 5** (a) Chemical structures of linear CO<sub>2</sub>-derived PHU and schematic diagram of intermolecular and intramolecular interactions of solid PHU. (b) PL spectra of solid PHU with different excitation wavelengths from 280 to 440 nm. (c) PL spectra of the white OLED fabricated by PHU and UV chip; (inset) PL spectra of the UV chip. (d) The CIE chromaticity coordinate of emission and luminescent photo of the white OLED. Figures are reproduced with permission from Ref. 92.

### 3 Multicomponent Strategy

Compared with single-component strategy, multicomponent strategy provides a facile way to achieve white-light emission based on luminescent materials with different colors.<sup>93,94</sup>

However, traditional multicomponent strategy is to mix fluorogens with several emissive colors (e.g., blue + green + red or green + yellow) together, especially for inorganic emitters. Besides, some systems based on organometallic emitters and an energy transfer process between two emitters were successfully achieved for white-light emission.<sup>95,96</sup> Hence, this method faces a severe challenge of phase separation, which makes them with a short lifetime, unstable color, and unexpected practical problems. Compared to inorganic and metal materials, pure organic molecules usually show better compatibility. Therefore, several methods such as trace doping, host-guest-based complexation, and cocrystallization can generate a homogeneous phase in the solid or aggregate state, which overcomes the

difficulties that multicomponent strategies faced. In this section, we will draw a mechanistic picture of those multicomponent strategies with typical examples.

#### 3.1 Doping

For organic AIEgens, it is possible to achieve full-color luminescence in the solid state by blending emitters with different colors. Moreover, flexible and similar conformation can increase the compatibility of the mixture. Zhu et al. synthesized three perchalcogenated arenes that contained O (Arene-O), S (Arene-S), and Se (Arene-Se) atoms and displayed blue, green, and red colors, respectively [Figs. 6(a)–6(d)].<sup>97</sup> The luminescence from Arene-S and Arene-Se was phosphorescence due to the heavy-atom effect, while that from Arene-O was assigned to fluorescence. The three luminescent primaries were utilized to construct a white-light emitter with a CIE coordinate of (0.27, 0.34) by incorporating them together with the molar

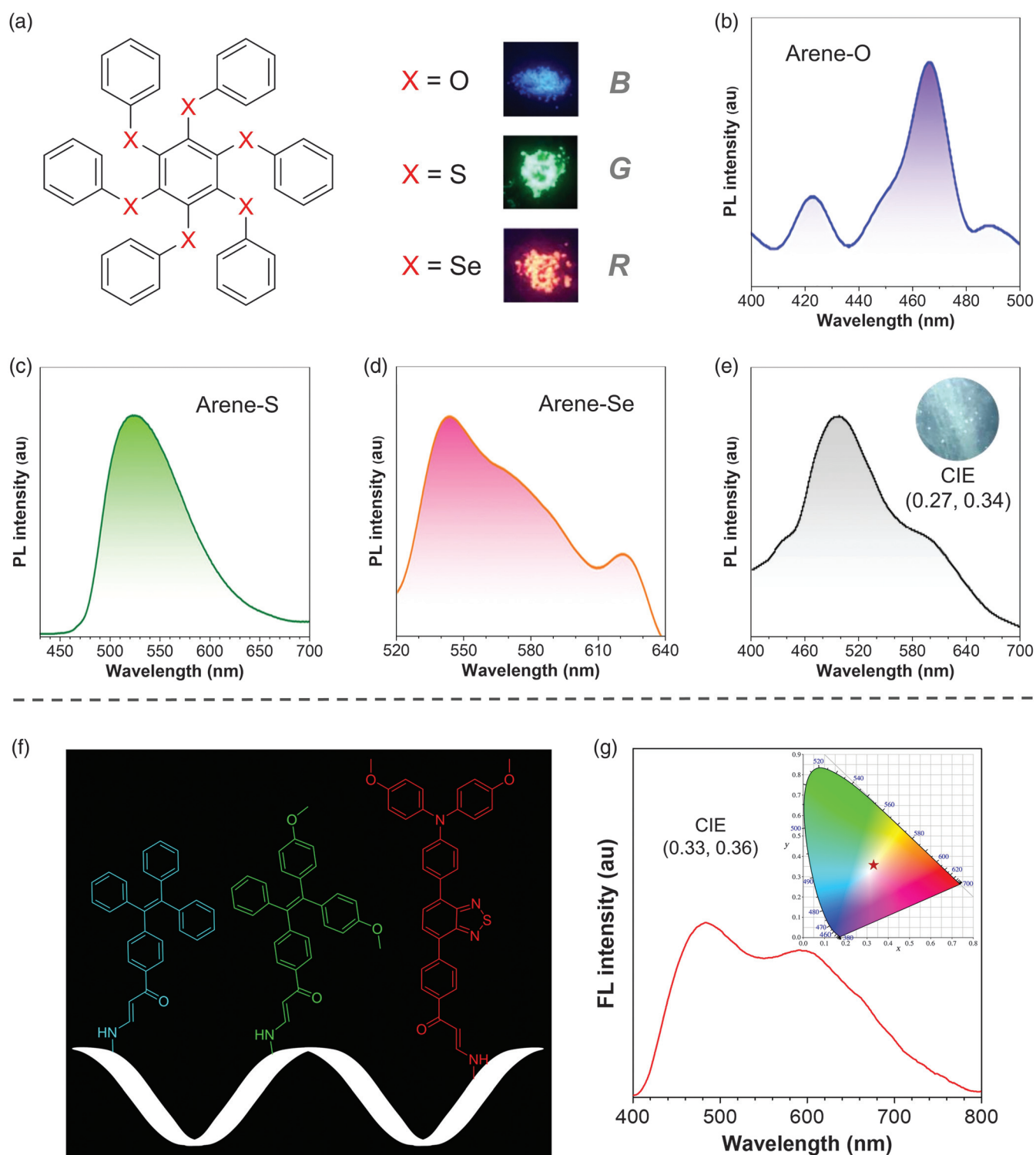


**Fig. 6** (a) Chemical structures and luminescent photos of the perchalcogenated arenes, where X stands for the element of O (Arene-O), S (Arene-S), and Se (Arene-Se), respectively. (b)–(d) PL spectra of three arenes in the solid state. (e) PL spectrum and luminescent photo of the solid mixture of Arene-O, Arene-S, Arene-Se with the molar ratio of 300:1:3. Figures are reproduced with permission from Ref. 97. (f) Chemical structure and preparation of white light-emitting silk through bioconjugation with TPE-pyo (blue), MTPEP-pyo (green), and MTPABP-pyo (red) at a molar ratio of 88:6:6. (g) PL spectrum and the CIE chromaticity coordinate of the fabricated white light-emitting silk. Figures are reproduced with permission from Ref. 98.

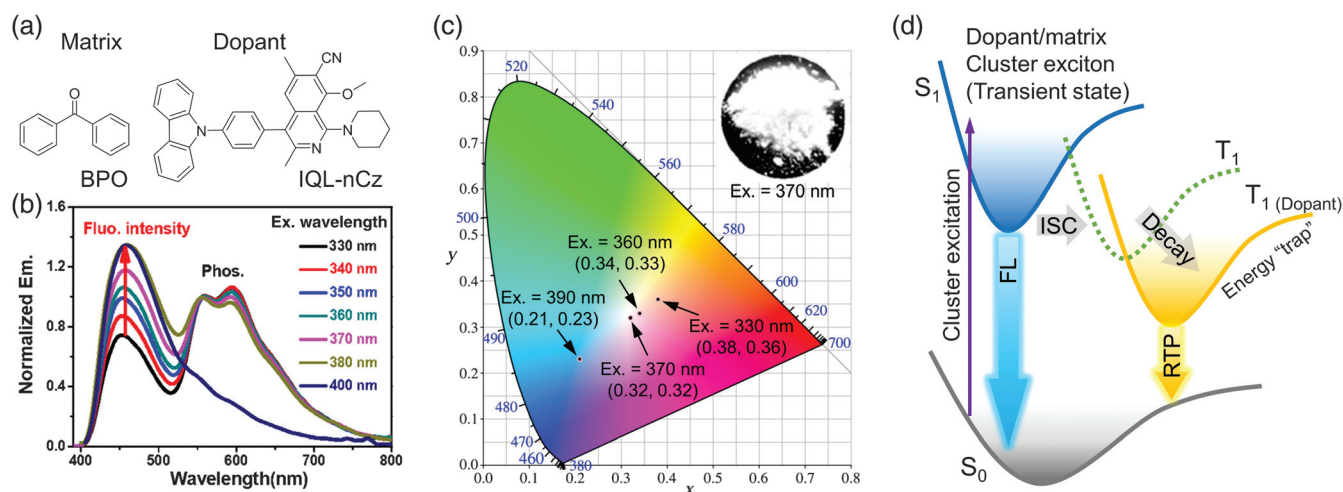


**Fig. 7** (a) Chemical structures of BPO as the matrix and IQL-nCz as the dopant. (b) PL spectra of the IQL-nCz/BPO-doped material with a molar ratio of 1:1000 under different excitation wavelengths. (c) The CIE chromaticity coordinate of the IQL-nCz/BPO-doped material under different excitation wavelength; (inset) luminescent photo taken under an excitation wavelength of 370 nm. Figures are reproduced with permission from Ref. 101. (d) Schematic mechanism of excitation and decay processes of this kind of dopant/matrix system. FL, fluorescence; ISC, intersystem crossing; RTP, room-temperature phosphorescence. Figures are reproduced with permission from Ref. 58.

ratio of 300:1:3 (Arene-O:Arene-S:Arene-Se) [Fig. 6(e)]. The powder X-ray diffraction spectra showed that the fabricated white emitter was crystalline, also indicating their good compatibility.

Apart from the above method of simply mixing multicolor materials to achieve full-color luminescence, incorporating multicolor fluorogens on a nonemissive matrix through chemical bonding provides another chance for white-light emitting materials. For instance, Tang et al. successfully fabricated white light-emitting silk through bioconjugation in 2021.<sup>98</sup> Three typical AIEgens (namely, TPE-pyo, MTPEP-pyo, and MTPABP-pyo) with three primary RGB colors were fixed in natural silks by chemical bonds formed between activated alkynes of AIEgens and amine groups of silks [Fig. 6(f)]. Each AIEgen emitted its intrinsic color in the fabricated silk and finally made up white-color emission with a CIE coordinate of (0.33, 0.36) [Fig. 6(g)]. Compared with traditional fluorescent dyes physically absorbed by the matrix, this doping method provides higher color retention and stability in the basic environment through chemical bonding, suggesting its potential advantages in silk fabrics and other applications utilized in harsh environments.

The doping strategy of two or more components also suggests a new insight on creating new photophysical behaviors that cannot be produced by themselves, which is different from utilizing their intrinsic luminescence as discussed above.<sup>58</sup> With the development of RTP from single-component organic molecules, trace dopant (even at part-per-billion level) in the non-RTP matrix plays a special role in producing new emissive species of RTP, resulting in dual emission of fluorescence and phosphorescence in such multicomponent systems.<sup>99,100</sup> It also creates a chance to realize white-light emission similar to the single-component system with features of fluorescence and phosphorescence. Based on this consideration, Lei et al. realized a white-light emitting material by doping IQL-nCz

(as the dopant) into benzophenone (BPO, as the matrix) with a molar ratio of 1:1000 [Fig. 7(a)].<sup>101</sup> In this system, the intrinsic fluorescence from the dopant located at 460 nm and a newly emerged phosphorescent peak located at 570 nm were observed, and the intensity ratio between two peaks was excitation-wavelength dependent [Fig. 7(b)]. Under excitation of a 370-nm UV lamp, a nearly pure white-light emission was noticed with a CIE coordinate of (0.32, 0.32) [Fig. 7(c)]. A general working scheme for this process is drawn in Fig 7(d). Due to multiple intermolecular interactions between the dopant and matrix, it was believed that an IQL-nCz molecule was surrounded by several BPO molecules and generated clusters. Upon excitation, these clusters are excited and form transient cluster excitons, as evidenced by the different excitation spectra of the doped material compared with that of dopant and matrix. Some excitons radiatively relax to the ground state from the central dopant in the form of fluorescence. In addition, through the ISC process and energy transfer from cluster to the dopant, other excitons rapidly decay to the more stable triplet state and the excited-state energy is finally “trapped” by the dopant, resulting in long-lifetime phosphorescent emission.<sup>58,102</sup> This doping method is now attracting more attention to extend the scope of RTP materials with functionality.<sup>103,104</sup>

### 3.2 Supramolecular Assembly

Inspired by nature, supramolecular assemblies have been rapidly developed as a great platform for advanced materials due to the well-defined conformation and fascinating topological structures, which are constructed by noncovalent intermolecular interactions. After adding functional units into the cavities of building blocks or utilizing building blocks with unique features, multifunctional host-guest systems can be constructed.<sup>105-107</sup> Therefore, the introduction of luminescent materials to the building blocks endows an opportunity to achieve white-light

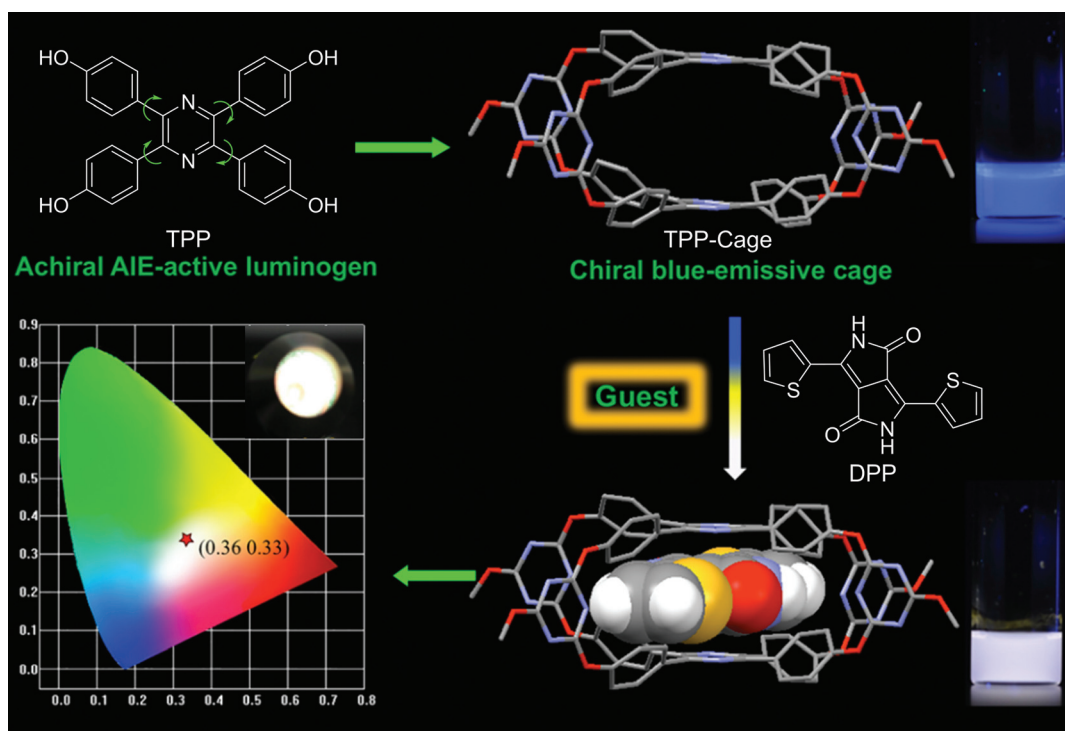


**Fig. 8** (Upper panel) Chemical structure of the AIE-active luminogen of TPP and crystal structure of chiral building block based on TPP. (Lower panel) Preparation of the DPP@TPP-Cage complex, crystal structure of DPP@TPP-Cage complex with white emission, and the CIE chromaticity coordinate of emission from DPP@TPP-Cage in poly(ethylene glycol) film deposited on a UV flashlight. Figures are reproduced with permission from Ref. 111.

emission, where the problem of phase separation of multi-component materials is also resolved by the regular-shaped packing in the solid state.<sup>108–110</sup> For example, a twisted and AIE-active tetraphenylpyrazine (TPP) structure was immobilized to construct the building blocks (TPP-Cage) that showed obvious chirality and blue emission in the solution state (Fig. 8).<sup>111</sup> Due to its large cavity, an ACQ-active diketopyrrolopyrrole (DPP) as the guest was encapsulated to form DPP@TPP-Cage complex. Since the  $\pi-\pi$  stacking was blocked by the TPP-Cage, DPP emitted yellow light in the cavity of such complexes. As a result, combining with the complementary blue color from the host of TPP-Cage, white-light emission was achieved in the aggregate and poly(ethylene glycol) film with a CIE coordinate of (0.36, 0.33). In addition, this fabricated white-light-emitting film exhibited good stability with its emission color hardly changing after placing at atmospheric conditions for 30 days. Similarly, Ni et al. reported a study on utilizing nonemissive cucurbituril[7] (Q[7]) and cucurbituril[8] (Q[8]) with different cavity sizes to anchor oligo(p-phenylenevinylene)-based cationic dye (G1). Q[7] was able to accommodate one G1 molecule and emitted blue color, while the cavity of Q[8] accommodated two molecules of the dye and produced yellow emission, respectively. Therefore, combining the above two complexes, white light-emitting with a CIE coordinate of (0.33, 0.36) was realized in this macrocycle-assisted supramolecular system.<sup>112</sup>

Since the structural diversity of guest and host molecules, supramolecular assembly becomes a platform for solid-state

white-light emitters (crystal, powder, film, hydrogel, etc.).<sup>106,113</sup> In addition, the white light of these host-guest systems originates not only from dual fluorescence but also from fluorescence and phosphorescence.<sup>114</sup>

### 3.3 Cocrystallization

Organic cocrystals, which are formed by two or more organic molecules with defined packing arrangements in the crystalline state, are gaining increased attention for crystal engineering and applications.<sup>115–118</sup> Apart from the sum of molecular properties, it is possible to create new chemical and physical behaviors through noncovalent intermolecular interactions (hydrogen bonding, halogen bonding,  $\pi-\pi$  interaction, etc.) within cocrystals. For example, researchers successfully utilized the strategy of cocrystals for transforming ACQ-active molecules to AIE active<sup>119–121</sup> and endowing cocrystals with self-healing and thermomechanical responses.<sup>122</sup> RTP is also realized within cocrystals through regulating excited states and the ISC process, which may give another way to realize white-light emission.<sup>123</sup>

With the consideration that halogen bonding can enhance the spin-orbital crossing (SOC), 1,4-diiodotetrafluorobenzene (DITFB) and 1,7-phenanthroline (PR) were used to build cocrystals with intermolecular halogen bonds.<sup>124</sup> Three crystals, namely P1D0, P2D1, and P1D1, contained an adjustable stoichiometric ratio between PR and DITFB of 1:0, 2:1, and 1:1, respectively, which displayed different emission properties under UV illumination. Especially, P2D1 produced white-light

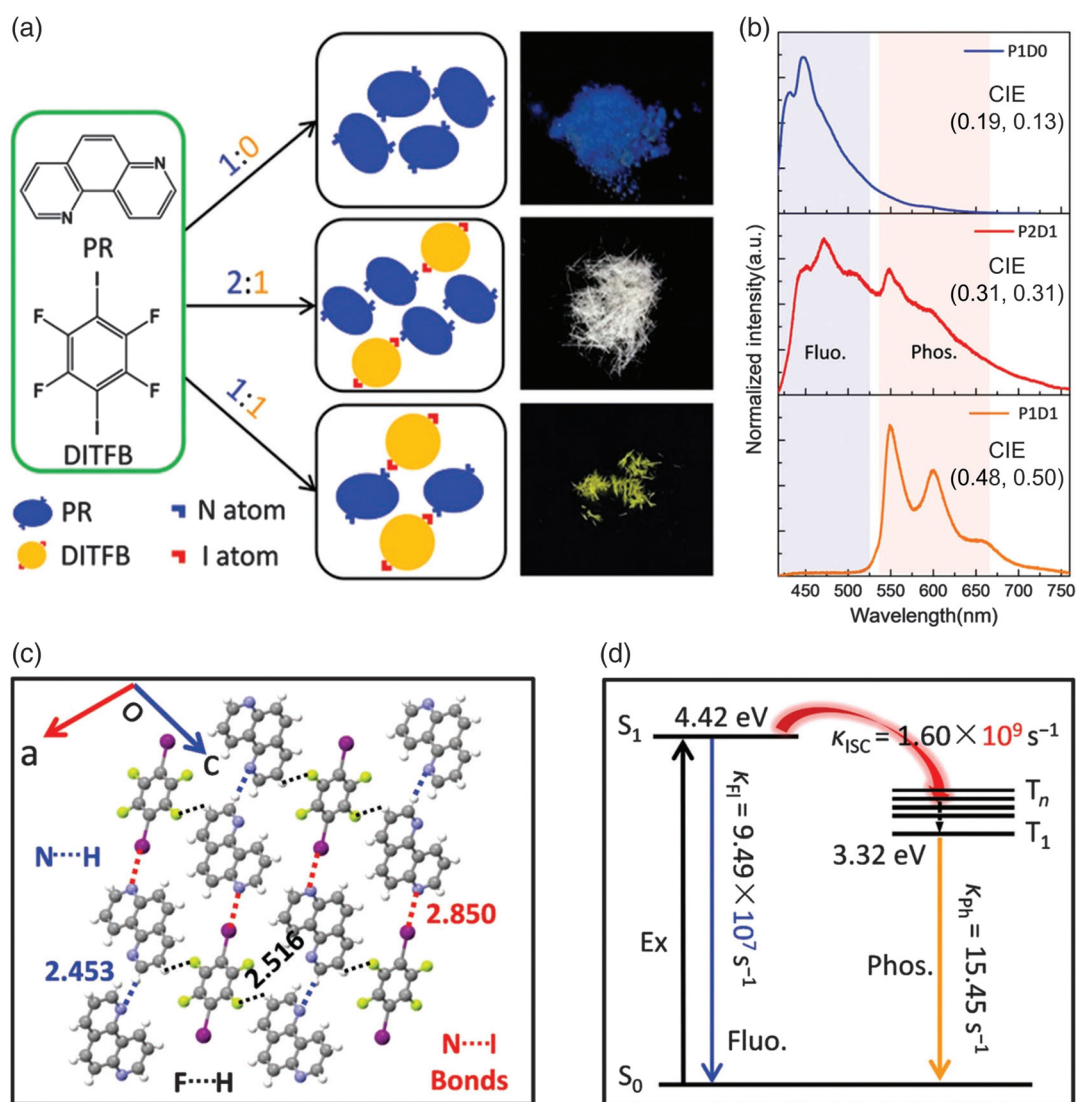


**Fig. 9** (a) Schematic illustration and luminescent photos of cocrystals formed by cocrystallization of PR and DITFB with molar ratios of 1:0 (P1D0), 2:1 (P2D1), and 1:1 (P1D1), respectively. (b) PL spectra of three cocrystals and their CIE chromaticity coordinates. (c) Single-crystal packing of P2D1 viewed along the *ac* plane. (d) Jablonski diagrams of P2D1 cocrystal with theoretically calculated energy levels and rate constants calculated from experimental data. Figures are reproduced with permission from Ref. 124.

emission in the crystalline state [Figs. 9(a) and 9(b)]. The PL spectra of P2D1 showed one fluorescent peak at 470 nm and another phosphorescent emission around 550 to 650 nm, which formed white light with a CIE coordinate of (0.31, 0.31). From crystal analysis of P2D1, it was obvious that each PR molecule connected with one DITFB through a strong N...I halogen bond and communicated with another DITFB through a comparatively weak H...F interaction, which finally helped to increase the strength of the SOC [Fig. 9(c)]. Those multiple intermolecular interactions also stabilized the excited state and promoted the small energy differences between the lowest singlet state ( $S_1$ ) and multitriplet states ( $T_n$ ). As a result, the rate of ISC ( $k_{ISC}$ ) of  $1.60 \times 10^9 \text{ s}^{-1}$  was nearly 16 times larger than the rate of fluorescence ( $k_{Fl}$ ) of  $9.49 \times 10^7 \text{ s}^{-1}$ . Cocrystal P2D1 finally displayed white-light emission with balanced fluorescence and phosphorescence [Fig. 9(d)]. On the contrary, P1D0 without

intermolecular halogen bonds only showed fluorescence, while P1D1 with much stronger halogen-bonding interactions and an SOC ability exhibited pure phosphorescent emission. By precisely modulating intermolecular interactions and excited states, cocrystallization is verified as a potential platform to generate homogeneous phases for white-light emission and optical applications.

#### 4 Applications of Organic White-light Aggregates

Along with the advances in design strategy and mechanistic elucidation of white-light emission from organic aggregates, much attention has been paid to the development of applications. Apart from white-light emission with adjustable color rendering index and color temperature, organic materials with luminescent

**Table 1** Summarized emission properties of all compounds mentioned in this review.

Strategy	Compound	State	Emission max. (nm)	Quantum (%)	CIE coordinate	Ref.
Dual fluorescence	DPAC-Tri( <i>o</i> 1,2)	Doped in polyTHF	435/610	6.8	(0.28, 0.25)	45
	<i>o</i> -CP	Crystal	410/557	46.0	(0.33, 0.36)	50
	CPzPO	Crystal/film	459/564	36.1	(0.31, 0.32)	53
Fluorescence and phosphorescence	TPO-Br	Crystal	434/549	36.6	(0.32, 0.33)	63
Dual phosphorescence	CIBDBT	Crystal	467/551	7.2	(0.33, 0.35)	81
Clusteroluminescence	PHU	Film	476/550	—	(0.33, 0.38)	92
Doping	Arene-O	Crystalline film	500/580	8.0	(0.27, 0.34)	97
	Arene-S			42.0 <sup>a</sup>		
	Arene-Se			21.0 <sup>a</sup>		
	TPE-pyo			14.1 <sup>b</sup>		
	MTPEP-pyo			22.2 <sup>b</sup>		
	MTPABP-pyo			6.6 <sup>b</sup>		
	IQL-nCz/BPO			Powder		
Supramolecular assembly	DPP@TPP-Cage	Aggregate or film in PEG	430/535	—	(0.36, 0.33)	111
	Q[7]/G1	Solid mixture	487/580	—	(0.33, 0.36)	112
	Q[8]/G1					
Cocrystallization	P1D1	Crystal	470/550	16.6	(0.31, 0.31)	124

<sup>a</sup>The absolute quantum yield of pure compound in the solid state.

<sup>b</sup>The absolute quantum yield of pure compound doped in natural silk.

<sup>c</sup>The absolute quantum yield of whole emission under excitation of 400 nm and phosphorescent emission under excitation of 370 nm.

properties in the aggregates also exhibited the advantages of low cost, excellent flexibility, compatibility, and environmental friendliness for practical applications. Here, some organic white-light emitters are highlighted for their potential values.

(1) Organic light-emitting diode (OLED): With the basic property of luminescence, luminescent materials are widely utilized on displaying, lighting, traffic, and flexible devices.<sup>125–128</sup> White-light emitters whose emissive color is close to natural sunlight are good candidates to construct white OLEDs. According to some strategies discussed in this review, single-component and multicomponent white OLEDs are fabricated.<sup>129</sup> For example, in consideration of the coexistence of two conformational isomers in the crystalline state, 2PQ–PTZ was verified as a white-light emitter. Therefore, it was utilized to fabricate a single-component white OLED with a maximum brightness of 6017 cd m<sup>-2</sup> and an external quantum efficiency of 10.12%.<sup>45</sup> A two-emissive-layered and nondoped white OLED was also fabricated based on two tetraphenylethene derivatives, namely TTPEPy and BTPETTD [Fig. 10(a)]. Two layers showed bluish-green and red color, respectively, and the final white-light device possessed a brightness of 18,000 cd m<sup>-2</sup> and an excellent color rendering index of 90.<sup>130</sup> Meanwhile, AIEgens-based OLEDs possess a reduced efficiency roll-off, and their emissive color can be easily adjusted through methods such as structural modification and device fabrication. Moreover, some white OLEDs are compatible with commercial devices and show great potential for wearable devices.<sup>132–134</sup>

(2) White luminescent dye: Compared with inorganic phosphors, organic molecules with functional groups can easily connect with other materials through chemical bonding. As a result,

white-emitting silk fabrics were successfully achieved through mixing natural silks with three dyes showing primary colors [Figs. 10(b), left].<sup>98</sup> The formed chemical bonds between silk fabrics and dyes endowed them with excellent color stability that was resistant to washing. Also, the flexibility of organic materials supports them as three-dimensional (3D) printing materials for the fabrication of some objectives with various shapes. As a demonstration, TPO-Br was utilized to build lampshades through 3D printing technology [Fig. 10(b), right].<sup>63</sup> In addition to bright white-light emission under UV lamps, this lampshade was transparent under daylight and showed a low weight.

(3) Circularly polarized luminescence (CPL): Some phenomena that are hardly accessible in isolated molecules would become obvious in the aggregate state, suggesting multifunctionality of aggregates such as bright emission, chirality, RTP, and delayed fluorescence.<sup>17</sup> CPL, as a key factor related to the origin of chirality, provides luminescence with another intriguing property of polarity.<sup>135</sup> For white-light emitters with CPL property, they can be widely utilized in advanced technologies including visible-light communication, data storage, 3D displays, etc. In 2019, Tang et al. developed a facile method to achieve CPL by incorporating achiral AIEgen, namely, 9,10-bis(diphenylmethylene)-9,10-dihydroanthracene (PDHA), with helical polymer poly(L-lactide) (PLLA). Due to the chiral nature of PLLA, the solid-state lamellae were left-handed twisting, and the formed spiral spherulites with a helical superstructure had an intrinsic ability for CPL modulation. In addition, amorphous and crystalline PDHA aggregates embedded in the polymer

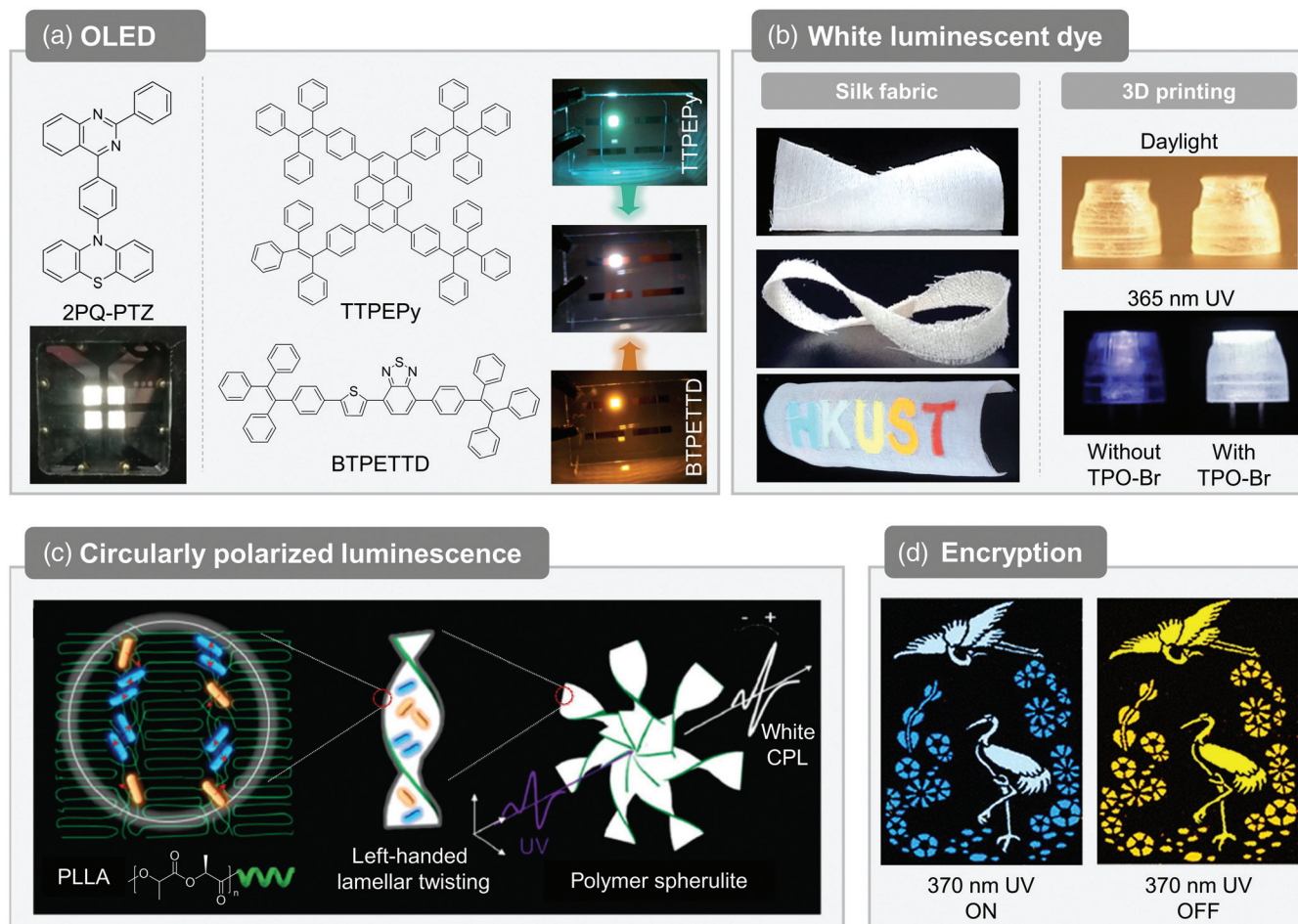


**Fig. 10** Examples of application of organic white-light emission materials. (a) (Left) Chemical structure of 2PQ-PTZ and device photo of a single-component OLED that is realized by conformational isomerization of 2PQ-PTZ. Figures are reproduced with permission from Ref. 45. (Right) Chemical structures of TTPEPy and BTPETTD and photos of an OLED constructed from them that shows green and red colors, respectively. The white OLED was constructed from two components of TTPEPy and BTPETTD with each thickness of 10 nm. Figures are reproduced with permission from Ref. 130. (b) (Left) White fluorescent silk fabric fabricated through bioconjugation between natural silk and AIEgens of TPE-pyo, MTPEP-pyo, and MTPABP-pyo. Figures are reproduced with permission from Ref. 98. (Right) Photos of 3D-printed lampshades without and with TPO-Br taken under daylight and 365 nm UV lamp. Figures are reproduced with permission from Ref. 63. (c) Schematic illustration of 3D spiral banded spherulite doped with PDHA aggregates and its mechanism for white CPL. Figures are reproduced with permission from Ref. 131. (d) Luminescent images drawn with IQL-Ph and IQL-TPA doped BPO under (left) and after (right) irradiation of a UV lamp with 370 nm wavelength, which can be utilized for information encryption. Figures are reproduced with permission from Ref. 101.

emitted yellow and blue light, finally resulting in white-light CPL [Fig. 10(c)].<sup>131</sup>

(4) Encryption: Information safety becomes more and more important with the development of the digital era. Light, as one kind of signal with versatile features, is a good candidate for the information transformation and anticounterfeiting. Emitters with dual fluorescence and phosphorescence are superior to traditional fluorescent materials since their two emissive channels have different colors and lifetime.<sup>54</sup> Therefore, many organic white-light emitters with RTP can fulfill the demand for high-level encryption. For instance, by mixing 0.1%

isoquinoline derivatives (IQL-Ph and IQL-TPA) into BPO, an organic-doped system was established with multiple properties of white-light emission, RTP, and excitation-dependent tunable color.<sup>101</sup> Two doped BPO materials were dissolved in solution for use as inks. As shown in Fig. 10(d), IQL-TPA/BPO was utilized to draw cranes and IQL-Ph/BPO was used for depicting flowers. The color of the two cranes was white under 370 nm excitation, while all flowers were cyan color. After ceasing the excitation source, all paintings showed a bright yellow after-glow. It demonstrates the potential capability of this doped system as writable ink for information encryption.

## 5 Conclusions and Perspectives

In this review, from the perspectives of single-component and multicomponent systems, we have discussed the recent progress of the development of white-light emission using organic molecules in the aggregate state. The key point is to produce polychromatic emissions simultaneously and balance the ratio between them to achieve white-light emission. From the viewpoint of a single-component strategy, organic aggregates with properties of dual fluorescence from two singlet states, balanced fluorescence and phosphorescence, dual phosphorescence with anti-Kasha's behavior, and clusteroluminescence were successfully utilized to achieve white-light emission. On the other hand, a multicomponent strategy, including doping, supramolecular assembly, and cocrystallization, synergistically combines several compounds for producing white light. Among all strategies, aggregate behavior plays a vital role: a rigid environment realized through intermolecular interactions in the aggregate state greatly blocks nonradiative decay and promotes radiative emission. Also, aggregate provides a platform for polychromatic luminescence and balanced emissions with different wavelengths to achieve white-light emission. Some unique photophysical behaviors, such as RTP, clusteroluminescence, and CPL, emerge in aggregates and provide more interesting phenomena and mechanistic insights. Therefore, apart from precise molecular design and synthesis, the behavior of organic molecules in the aggregate state should be carefully considered in future work, including structure–property relationship at the aggregate level, characterization, and control of aggregate morphology.

We also highlighted some advanced applications of white-light emission from organic aggregates, showing potentials for next-generation luminescent materials. Single-component strategy and good compatibility of multicomponent strategy resolve the challenge of phase separation of traditional inorganic materials. In addition, the flexibility of organic materials indicates their potential applications on flexible devices, which may further endow them with applications for display and illumination.<sup>136,137</sup> Although many successes of pure organic white-light emitters have been achieved, their performance is still far behind those inorganic and organometallic emitters in terms of brightness, efficiency, quality of color, device fabrication, etc. In addition, due to their morphology-dependent properties, the control and optimization of morphology during device fabrication and application is another consideration. Therefore, they are far from being widely utilized in our daily life, and many existing issues need to be further addressed.

Last, but not least, the development of modern computational methodologies makes it possible to illustrate photophysical processes of single molecules and aggregates, providing mechanistic understandings and rational design of white-light emitters. However, as the diagram shifts from molecular science to aggregate science, present computational methods are unable to accurately describe inherent luminescent mechanisms at the level of aggregate, especially for intermolecular interactions and electron delocalization. From this perspective, multiscale computational approaches and even artificial intelligence technology are needed to dig the nature of aggregates and extend the scope of organic white-light emitters. As a branch of aggregate science, organic aggregates with white-light emission show their values for advanced materials and underlying mechanisms of photophysics. We believe that the future road for practical applications is challenging and rewarding.

## Acknowledgments

This work was partially supported by the National Natural Science Foundation of China (21788102), the Research Grants Council of Hong Kong (16305518, 16307020, C6014-20W, C6009-17G, and 16305618), the Innovation and Technology Commission (ITC-CNERC14SC01), and the Natural Science Foundation of Guangdong Province (2019B121205002). H. Z is thankful for the support from the Fundamental Research Funds for the Central Universities (2021QNA4032), the Open Fund of Guangdong Provincial Key Laboratory of Luminescence from Molecular Aggregates, and the South China University of Technology (2019B030301003).

## References

1. J. Cho et al., "White light-emitting diodes: history, progress, and future," *Laser Photonics Rev.* **11**(2), 1600147 (2017).
2. E. F. Schubert and J. K. Kim, "Solid-state light sources getting smart," *Science* **308**(5726), 1274–1278 (2005).
3. X. Li et al., "A high efficacy and tunable white light-emitting diode cluster with both color fidelity and nonvisual performances close to natural lights," *Color Res. Appl.* **45**(6), 1067–1075 (2020).
4. S. Ye et al., "Phosphors in phosphor-converted white light-emitting diodes: recent advances in materials, techniques and properties," *Mater. Sci. Eng. R Rep.* **71**(1), 1–34 (2010).
5. H. Zhang, Q. Su, and S. Chen, "Quantum-dot and organic hybrid tandem light-emitting diodes with multi-functionality of full-color-tunability and white-light-emission," *Nat. Commun.* **11**(1), 2826 (2020).
6. S. Nakamura et al., "Superbright green InGaN single-quantum-well-structure light-emitting diodes," *Jpn. J. Appl. Phys.* **34**, L1332–L1335 (1995).
7. M. D. Smith and H. I. Karunadasa, "White-light emission from layered halide perovskites," *Acc. Chem. Res.* **51**(3), 619–627 (2018).
8. T. Pulli et al., "Advantages of white LED lamps and new detector technology in photometry," *Light Sci. Appl.* **4**(9), e332 (2015).
9. P. Schlotter, R. Schmidt, and J. Schneider, "Luminescence conversion of blue light emitting diodes," *Appl. Phys. A* **64**(4), 417–418 (1997).
10. C.-Y. Sun et al., "Efficient and tunable white-light emission of metal–organic frameworks by iridium-complex encapsulation," *Nat. Commun.* **4**(1), 2717 (2013).
11. X. Zhao et al., "Metallophilicity-induced clusterization: single-component white-light clusteroluminescence with stimulus response," *CCS Chem.* **3**, 3039–3049 (2021).
12. D. Tu et al., "How do molecular motions affect structures and properties at molecule and aggregate levels?" *J. Am. Chem. Soc.* **143**(30), 11820–11827 (2021).
13. E. Merritt, "The relation between intensity of fluorescence and concentration in solid solutions," *J. Opt. Soc. Am.* **12**(6), 613–622 (1926).
14. W. F. Watson and R. Livingston, "Concentration quenching of fluorescence in chlorophyll solutions," *Nature* **162**(4116), 452–453 (1948).
15. J. Luo et al., "Aggregation-induced emission of 1-methyl-1,2,3,4,5-pentaphenylsilole," *Chem. Commun.* **18**(18), 1740–1741 (2001).
16. H. Zhang et al., "Aggregate science: from structures to properties," *Adv. Mater.* **32**(36), 2001457 (2020).
17. Z. Zhao et al., "Aggregation-induced emission: new vistas at aggregate level," *Angew. Chem. Int. Ed.* **59**(25), 9888–9907 (2020).
18. J. Yang, M. Fang, and Z. Li, "Organic luminescent materials: the concentration on aggregates from aggregation-induced emission," *Aggregate* **1**(1), 6–18 (2020).

19. Y. Tu et al., "Aggregate science: much to explore in the meso world," *Matter* **4**(2), 338–349 (2021).
20. W. Xu, D. Wang, and B. Z. Tang, "NIR-II AIEgens: a win–win integration towards bioapplications," *Angew. Chem. Int. Ed.* **60**(14), 7476–7487 (2021).
21. J. Zhang et al., "Stimuli-responsive AIEgens," *Adv. Mater.* **33**(32), 2008071 (2021).
22. Y. Wang et al., "Sugar-based aggregation-induced emission luminogens: design, structures, and applications," *Chem. Rev.* **120**(10), 4537–4577 (2020).
23. Z. Li et al., "Aggregation-induced emission-active gels: fabrications, functions, and applications," *Adv. Mater.* **33**(33), 2100021 (2021).
24. S. Ma et al., "Organic molecular aggregates: from aggregation structure to emission property," *Aggregate* **2**(4), e96 (2021).
25. M. Yu et al., "Promising applications of aggregation-induced emission luminogens in organic optoelectronic devices," *Photonix* **1**(1), 11 (2020).
26. S. Xu, Y. Duan, and B. Liu, "Precise molecular design for high-performance luminogens with aggregation-induced emission," *Adv. Mater.* **32**(1), 1903530 (2020).
27. J. Kido, M. Kimura, and K. Nagai, "Multilayer white light-emitting organic electroluminescent device," *Science* **267**(5202), 1332–1334 (1995).
28. S. Reineke et al., "White organic light-emitting diodes with fluorescent tube efficiency," *Nature* **459**(7244), 234–238 (2009).
29. H. Wang et al., "Positive/negative phototropism: controllable molecular actuators with different bending behavior," *CCS Chem.* **3**(4), 1491–1500 (2020).
30. Y. Tu et al., "Mechanistic connotations of restriction of intramolecular motions (RIM)," *Natl. Sci. Rev.* **8**, nwa260 (2020).
31. J. Zhang et al., "Restriction of intramolecular motion (RIM): investigating AIE mechanism from experimental and theoretical studies," *Chem. Res. Chin. Univ.* **37**(1), 1–15 (2021).
32. Q. Peng and Z. Shuai, "Molecular mechanism of aggregation-induced emission," *Aggregate* **2**(5), e91 (2021).
33. H. Shen et al., "Photodegradation-induced turn-on luminescence of tetraphenylethylene-based trithiocarbonate polymers," *Chin. J. Chem.* **39**(10), 2837–2842 (2021).
34. Z. Chen et al., "Single-molecular white-light emitters and their potential WOLED applications," *Adv. Mater.* **32**(11), 1903269 (2020).
35. B. Roy et al., "All in one: stimuli-responsive, efficient mitottracking, and single source white light emission," *J. Phys. Chem. Lett.* **12**(4), 1162–1168 (2021).
36. Y. Tu et al., "An intelligent AIEgen with nonmonotonic multi-responses to multistimuli," *Adv. Sci.* **7**(20), 2001845 (2020).
37. Y. Yang et al., "An organic white light-emitting fluorophore," *J. Am. Chem. Soc.* **128**(43), 14081–14092 (2006).
38. M. Kasha, "Characterization of electronic transitions in complex molecules," *Discuss. Faraday Soc.* **9**, 14–19 (1950).
39. H. Wang et al., "A new strategy for achieving single-molecular white-light emission: using vibration-induced emission (VIE) plus aggregation-induced emission (AIE) mechanisms as a two-pronged approach," *Chem. Commun.* **55**(13), 1879–1882 (2019).
40. D. Tu et al., "Highly emissive organic single-molecule white emitters by engineering o-carborane-based luminophores," *Angew. Chem. Int. Ed.* **56**(38), 11370–11374 (2017).
41. Z. Xie et al., "Hydrogen-bonding-assisted intermolecular charge transfer: a new strategy to design single-component white-light-emitting materials," *Adv. Funct. Mater.* **27**(47), 1703918 (2017).
42. K.-C. Tang et al., "Fine tuning the energetics of excited-state intramolecular proton transfer (ESIPT): white light generation in a single ESIPT system," *J. Am. Chem. Soc.* **133**(44), 17738–17745 (2011).
43. H. Liu et al., "ESIPT-active organic compounds with white luminescence based on crystallization-induced keto emission (CIKE)," *Chem. Commun.* **53**(55), 7832–7835 (2017).
44. Y. Chen et al., "Color-tunable and ESIPT-inspired solid fluorophores based on benzothiazole derivatives: aggregation-induced emission, strong solvatochromic effect, and white light emission," *ACS Appl. Mater. Interfaces* **12**(49), 55094–55106 (2020).
45. B. Li et al., "Realizing efficient single organic molecular white light-emitting diodes from conformational isomerization of quinoxaline-based emitters," *ACS Appl. Mater. Interfaces* **12**(12), 14233–14243 (2020).
46. S. Samanta, U. Manna, and G. Das, "White-light emission from simple AIE-ESIPT-excimer tripled single molecular system," *New J. Chem.* **41**(3), 1064–1072 (2017).
47. N. A. Kukhta and M. R. Bryce, "Dual emission in purely organic materials for optoelectronic applications," *Mater. Horiz.* **8**(1), 33–55 (2021).
48. J. Chatsirisupachai et al., "Unique dual fluorescence emission in the solid state from a small molecule based on phenanthrocarbazole with an AIE luminogen as a single-molecule white-light emissive material," *Mater. Chem. Front.* **5**(5), 2361–2372 (2021).
49. X. Chen et al., "Nondoped red fluorophores with hybridized local and charge-transfer state for high-performance fluorescent white organic light-emitting diodes," *ACS Appl. Mater. Interfaces* **11**(42), 39026–39034 (2019).
50. X. Feng et al., "Dual fluorescence of tetraphenylethylene-substituted pyrenes with aggregation-induced emission characteristics for white-light emission," *Chem. Sci.* **9**(25), 5679–5687 (2018).
51. A. Mangini, *Advances in Molecular Spectroscopy Volume 2: Proceedings of the Fourth International Meeting On Molecular Spectroscopy*, Pergamon Press, Oxford, Symposium Publications Division (1962).
52. Y. Gao et al., "Hybridization and de-hybridization between the locally-excited (LE) state and the charge-transfer (CT) state: a combined experimental and theoretical study," *Phys. Chem. Chem. Phys.* **18**(35), 24176–24184 (2016).
53. H. Shen, Y. Li, and Y. Li, "Self-assembly and tunable optical properties of intramolecular charge transfer molecules," *Aggregate* **1**(1), 57–68 (2020).
54. W. Zhao, Z. He, and B. Z. Tang, "Room-temperature phosphorescence from organic aggregates," *Nat. Rev. Mater.* **5**(12), 869–885 (2020).
55. H. Gao and X. Ma, "Recent progress on pure organic room temperature phosphorescent polymers," *Aggregate* **2**(4), e38 (2021).
56. P. Alam et al., "Two are better than one: a design principle for ultralong-persistent luminescence of pure organics," *Adv. Mater.* **32**(22), 2001026 (2020).
57. H. Tian et al., "Molecular engineering for metal-free amorphous room-temperature phosphorescent materials," *Angew. Chem. Int. Ed.* **59**(28), 11206–11216 (2019).
58. X. Zhang et al., "Ultralong UV/mechano-excited room temperature phosphorescence from purely organic cluster excitons," *Nat. Commun.* **10**(1), 5161 (2019).
59. Y. Sun et al., "Management of singlet and triplet excitons for efficient white organic light-emitting devices," *Nature* **440**(7086), 908–912 (2006).
60. M. Shimizu and T. Sakurai, "Metal-free organic luminophores that exhibit dual fluorescence and phosphorescence emission at room temperature," *ChemPlusChem* **86**(3), 446–459 (2021).
61. J. A. Li et al., "Transient and persistent room-temperature mechanoluminescence from a white-light-emitting AIEgen with tricolor emission switching triggered by light," *Angew. Chem. Int. Ed.* **57**(22), 6449–6453 (2018).
62. P. She et al., "Controlling organic room temperature phosphorescence through external heavy-atom effect for white light emission and luminescence printing," *Adv. Opt. Mater.* **8**(4), 1901437 (2019).
63. J. Wang et al., "A facile strategy for realizing room temperature phosphorescence and single molecule white light emission," *Nat. Commun.* **9**(1), 2963 (2018).

64. T. Smith and J. Guild, "The C.I.E. colorimetric standards and their use," *Trans. Opt. Soc.* **33**(3), 73–134 (1931).
65. Y. Wen et al., "Modulating room temperature phosphorescence by oxidation of thianthrene to achieve pure organic single-molecule white-light emission," *CCS Chem.* **3**(7), 1940–1948 (2020).
66. B. Xu et al., "White-light emission from a single heavy atom-free molecule with room temperature phosphorescence, mechanochromism and thermochromism," *Chem. Sci.* **8**(3), 1909–1914 (2017).
67. S. Cai et al., "Enhancing ultralong organic phosphorescence by effective  $\pi$ -type halogen bonding," *Adv. Funct. Mater.* **28**(9), 1705045 (2018).
68. L. Xiao and H. Fu, "Enhanced room-temperature phosphorescence through intermolecular halogen/hydrogen bonding," *Chem. Eur. J.* **25**(3), 714–723 (2019).
69. Y. Wen et al., "One-dimensional  $\pi$ - $\pi$  stacking induces highly efficient pure organic room-temperature phosphorescence and ternary-emission single-molecule white light," *J. Mater. Chem. C* **7**(40), 12502 (2019).
70. S. Cai et al., "Hydrogen-bonded organic aromatic frameworks for ultralong phosphorescence by intralayer  $\pi$ - $\pi$  interactions," *Angew. Chem. Int. Ed.* **57**(15), 4005–4009 (2018).
71. C. Zhou et al., "Ternary emission of fluorescence and dual phosphorescence at room temperature: a single-molecule white light emitter based on pure organic aza-aromatic material," *Adv. Funct. Mater.* **28**(32), 1802407 (2018).
72. W. Z. Yuan et al., "Crystallization-induced phosphorescence of pure organic luminogens at room temperature," *J. Phys. Chem. C* **114**(13), 6090–6099 (2010).
73. M. Beer and H. C. Longuet-Higgins, "Anomalous light emission of azulene," *J. Chem. Phys.* **23**(8), 1390–1391 (1955).
74. J. C. Del Valle and J. Catalan, "Kasha's rule: a reappraisal," *Phys. Chem. Chem. Phys.* **21**(19), 10061–10069 (2019).
75. T. Itoh, "Fluorescence and phosphorescence from higher excited states of organic molecules," *Chem. Rev.* **112**(8), 4541–4568 (2012).
76. L. Shi et al., "De novo strategy with engineering anti-Kasha/Kasha fluorophores enables reliable ratiometric quantification of biomolecules," *Nat. Commun.* **11**(1), 793 (2020).
77. Y. Zhou et al., "Anti-Kasha's rule emissive switching induced by intermolecular H-bonding," *Chem. Mater.* **30**(21), 8008–8016 (2018).
78. T. Wang et al., "Aggregation-induced dual-phosphorescence from organic molecules for nondoped light-emitting diodes," *Adv. Mater.* **31**(51), 1904273 (2019).
79. D. Chaudhuri et al., "Metal-free OLED triplet emitters by side-stepping Kasha's rule," *Angew. Chem. Int. Ed.* **52**(50), 13449–13452 (2013).
80. T. Itoh, "Successive occurrence of the T1( $\pi$ ,  $\pi^*$ ) and T2( $n$ ,  $\pi^*$ ) phosphorescence and the S1( $n$ ,  $\pi^*$ ) fluorescence observed for p-cyanobenzaldehyde in a solid matrix," *J. Lumin.* **109**(3), 221–225 (2004).
81. Z. He et al., "White light emission from a single organic molecule with dual phosphorescence at room temperature," *Nat. Commun.* **8**(1), 416 (2017).
82. J. Zhang et al., "How to manipulate through-space conjugation and clusteroluminescence of simple AIEgens with isolated phenyl rings," *J. Am. Chem. Soc.* **143**(25), 9565–9574 (2021).
83. Z. Wang et al., "Recent advances in clusteroluminescence," *Top. Curr. Chem.* **379**(2), 14 (2021).
84. B. He et al., "Clusteroluminescence from cluster excitons in small heterocyclics free of aromatic rings," *Adv. Sci.* **8**(7), 2004299 (2021).
85. H. Zhang et al., "Clusterization-triggered emission: uncommon luminescence from common materials," *Mater. Today* **32**, 275–292 (2019).
86. H. Zhang et al., "Why do simple molecules with 'isolated' phenyl rings emit visible light?" *J. Am. Chem. Soc.* **139**(45), 16264–16272 (2017).
87. Z. Zhao et al., "Revisiting an ancient inorganic aggregation-induced emission system: an enlightenment to clusteroluminescence," *Aggregate* **2**(2), e36 (2021).
88. Z. Zhou et al., "Achieving white-light emission in a single-component polymer with halogen-assisted interaction," *Sci. China Chem.* **64**(3), 467–477 (2021).
89. B. Liu et al., "Clustering-induced white light emission from carbonized polymer dots," *Adv. Photonics Res.* **2**(5), 2000161 (2021).
90. C. Shang et al., "Orange-red and white-emitting nonconventional luminescent polymers containing cyclic acid anhydride and lactam groups," *J. Mater. Chem. C* **8**(3), 1017–1024 (2020).
91. Y. Shi et al., "Carbon dots: an innovative luminescent nanomaterial," *Aggregate*, e108 (2021).
92. B. Liu et al., "Fluorescent linear CO<sub>2</sub>-derived poly(hydroxyurethane) for cool white LED," *J. Mater. Chem. C* **5**(20), 4892–4898 (2017).
93. H. Dong et al., "Organic composite materials: understanding and manipulating excited states toward higher light-emitting performance," *Aggregate* **2**(4), e103 (2021).
94. L. Zhang et al., "Covalent organic frameworks for optical applications," *Aggregate* **2**(3), e24 (2021).
95. N. Hendlar et al., "Efficient separation of dyes by mucin: toward bioinspired white-luminescent devices," *Adv. Mater.* **23**(37), 4261–4264 (2011).
96. A. Rizzo et al., "White light with phosphorescent protein fibrils in OLEDs," *Nano Lett.* **10**(6), 2225–2230 (2010).
97. T. Weng et al., "A fluorescence-phosphorescence-phosphorescence triple-channel emission strategy for full-color luminescence," *Small* **16**(7), 1906475 (2020).
98. C. Liu et al., "Functionalization of silk by AIEgens through facile bioconjugation: full-color fluorescence and long-term bioimaging," *Angew. Chem. Int. Ed.* **60**(22), 12424–12430 (2021).
99. C. Chen et al., "Carbazole isomers induce ultralong organic phosphorescence," *Nat. Mater.* **20**(2), 175–180 (2021).
100. B. Chen et al., "Organic guest-host system produces room-temperature phosphorescence at part-per-billion level," *Angew. Chem. Int. Ed.* **60**(31), 16970–16973 (2021).
101. D. Wang et al., "Excitation-dependent triplet-singlet intensity from organic host-guest materials: tunable color, white-light emission, and room-temperature phosphorescence," *J. Phys. Chem. Lett.* **12**(7), 1814–1821 (2021).
102. R. Kabe and C. Adachi, "Organic long persistent luminescence," *Nature* **550**(7676), 384–387 (2017).
103. Y. Lei et al., "Wide-range color-tunable ultralong organic phosphorescence materials for printable and writable security inks," *Angew. Chem. Int. Ed.* **59**(37), 16054–16060 (2020).
104. S. Sun et al., "A universal strategy for organic fluid phosphorescence materials," *Angew. Chem. Int. Ed.* **60**(34), 18557–18560 (2021).
105. H.-T. Feng, J. W. Y. Lam, and B. Z. Tang, "Self-assembly of AIEgens," *Coord. Chem. Rev.* **406**, 213142 (2020).
106. Q. Zhao et al., "Tunable white-light emission by supramolecular self-sorting in highly swollen hydrogels," *Chem. Commun.* **54**(2), 200–203 (2018).
107. X.-Y. Lou and Y.-W. Yang, "Aggregation-induced emission systems involving supramolecular assembly," *Aggregate* **1**(1), 19–30 (2020).
108. H.-L. Yang et al., "Metal-free white light-emitting fluorescent material based on simple pillar[5]arene-tripodal amide system and theoretical insights on its assembly and fluorescent properties," *Langmuir* **36**(45), 13469–13476 (2020).
109. T. Xiao et al., "An efficient artificial light-harvesting system with tunable emission in water constructed from a H-bonded AIE supramolecular polymer and Nile red," *Chem. Commun.* **56**(80), 12021–12024 (2020).
110. M. Louis et al., "Blue-light-absorbing thin films showing ultralong room-temperature phosphorescence," *Adv. Mater.* **31**(12), 1807887 (2019).

111. H.-T. Feng et al., "White-light emission of a binary light-harvesting platform based on an amphiphilic organic cage," *Chem. Mater.* **30**(4), 1285–1290 (2018).
112. Y. Xia, S. Chen, and X.-L. Ni, "White light emission from cucurbituril-based host-guest interaction in the solid state: new function of the macrocyclic host," *ACS Appl. Mater. Interfaces* **10**(15), 13048–13052 (2018).
113. G. Sun et al., "Supramolecular assembly-driven color-tuning and white-light emission based on crown-ether-functionalized dihydrophenazine," *ACS Appl. Mater. Interfaces* **12**(9), 10875–10882 (2020).
114. J. J. Li et al., "Room-temperature phosphorescence and reversible white light switch based on a cyclodextrin polypseudorotaxane xerogel," *Adv. Opt. Mater.* **7**(20), 1900589 (2019).
115. L. Sun et al., "Cocrystal engineering: a collaborative strategy toward functional materials," *Adv. Mater.* **31**(39), 1902328 (2019).
116. W. Zhu et al., "Rational design of charge-transfer interactions in halogen-bonded co-crystals toward versatile solid-state optoelectronics," *J. Am. Chem. Soc.* **137**(34), 11038–11046 (2015).
117. X. Deng et al., "Our research progress in heteroaggregation and homoaggregation of organic  $\pi$ -conjugated systems," *Aggregate* **2**(3), e35 (2021).
118. Y. Huang et al., "Organic cocrystals: beyond electrical conductivities and field-effect transistors (FETs)," *Angew. Chem. Int. Ed.* **58**(29), 9696–9711 (2019).
119. H. Wang et al., "Visualization and manipulation of solid-state molecular motions in cocrystallization processes," *J. Am. Chem. Soc.* **143**(25), 9468–9477 (2021).
120. Y. Huang et al., "Reducing aggregation caused quenching effect through co-assembly of PAH chromophores and molecular barriers," *Nat. Commun.* **10**(1), 169 (2019).
121. Y. Huang et al., "Green grinding-coassembly engineering toward intrinsically luminescent tetracene in cocrystals," *ACS Nano* **14**(11), 15962–15972 (2020).
122. G. Liu et al., "Self-healing behavior in a thermo-mechanically responsive cocrystal during a reversible phase transition," *Angew. Chem. Int. Ed.* **56**(1), 198–202 (2017).
123. S. d'Agostino et al., "Tipping the balance with the aid of stoichiometry: room temperature phosphorescence versus fluorescence in organic cocrystals," *Cryst. Growth Des.* **15**(4), 2039–2045 (2015).
124. C. Feng et al., "Excited-state modulation for controlling fluorescence and phosphorescence pathways toward white-light emission," *Adv. Opt. Mater.* **7**(20), 1900767 (2019).
125. N. T. Kalyani and S. J. Dhoble, "Organic light emitting diodes: energy saving lighting technology: a review," *Renew. Sust. Energ. Rev.* **16**(5), 2696–2723 (2012).
126. S. Shao and L. Wang, "Through-space charge transfer polymers for solution-processed organic light-emitting diodes," *Aggregate* **1**(1), 45–56 (2020).
127. T. Yu et al., "Progress in small-molecule luminescent materials for organic light-emitting diodes," *Sci. China Chem.* **58**(6), 907–915 (2015).
128. T. Zhang et al., "'Simple' aggregation-induced emission luminogens for nondoped solution-processed organic light-emitting diodes with emission close to pure red in the standard red, green, and blue gamut," *Adv. Photonics Res.* **2**(6), 2100004 (2021).
129. Z. Zhao, J. W. Y. Lam, and B. Z. Tang, "Tetraphenylethene: a versatile AIE building block for the construction of efficient luminescent materials for organic light-emitting diodes," *J. Mater. Chem.* **22**(45), 23726–23740 (2012).
130. S. Chen et al., "Non-doped white organic light-emitting diodes based on aggregation-induced emission," *J. Phys. D Appl. Phys.* **43**(9), 095101 (2010).
131. Y. Cheng et al., "Facile emission color tuning and circularly polarized light generation of single luminogen in engineering robust forms," *Mater. Horiz.* **6**(2), 405–411 (2019).
132. Y. Jeon et al., "Parallel-stacked flexible organic light-emitting diodes for wearable photodynamic therapeutics and color-tunable optoelectronics," *ACS Nano* **14**(11), 15688–15699 (2020).
133. J. H. Koo et al., "Wearable electrocardiogram monitor using carbon nanotube electronics and color-tunable organic light-emitting diodes," *ACS Nano* **11**(10), 10032–10041 (2017).
134. H. Ding et al., "An AIEgen-based 3D covalent organic framework for white light-emitting diodes," *Nat. Commun.* **9**(1), 5234 (2018).
135. C. Liu et al., "Chiral assembly of organic luminogens with aggregation-induced emission," *Chem. Sci.* (2022).
136. Y. Li et al., "Implantable bioelectronics toward long-term stability and sustainability," *Matter* **4**(4), 1125–1141 (2021).
137. X. Shi et al., "Large-area display textiles integrated with functional systems," *Nature* **591**(7849), 240–245 (2021).

**Jianyu Zhang** received his bachelor's degree in science from Sun Yat-sen University in 2019. He is currently a PhD candidate in the Department of Chemistry at The Hong Kong University of Science and Technology (HKUST) under the supervision of Professor Ben Zhong Tang. His research interests focus on the photophysical mechanism, computational chemistry, aggregation-induced emission, and clusteroluminescence.

**Xueqian Zhao** received his PhD from HKUST in 2021 under the supervision of Professor Ben Zhong Tang. He is now conducting his postdoctoral work on the development of functional luminescent materials with AIE characteristics and exploration of their biological applications in Professor Sijie Chen's laboratory at Ming Wai Lau Centre for Reparative Medicine, Karolinska Institutet.

**Hanchen Shen** received his bachelor's degree in pharmacy from Fudan University in 2020. He is currently a PhD student under the supervision of Professor Ben Zhong Tang in the Department of Chemistry, HKUST. His research mainly focuses on the biomedical applications of multifunction fluorescent materials.

**Jacky W. Y. Lam** received his PhD from HKUST in 2003 under the supervision of Professor Ben Zhong Tang. He is currently a research associate professor in the Department of Chemistry at HKUST. His research interests include macromolecular chemistry and materials science.

**Haoke Zhang** is an assistant professor at Zhejiang University. He received his PhD from HKUST in 2018 under the supervision of Professor Ben Zhong Tang. His research interests focus on photophysical chemistry, chiral chemistry, and computational chemistry.

**Ben Zhong Tang** works as a distinguished presidential chair professor at The Chinese University of Hong Kong, Shenzhen (CUHK-SZ), dean of the School of Science and Engineering at CUHK-SZ, director of AIE Institute. He received his BS and PhD degrees from South China University of Technology and Kyoto University, respectively. He conducted postdoctoral study at the University of Toronto. His research interests include materials science, macromolecular chemistry, and biomedical theranostics. His lab is spearheading research on aggregation-induced emission.